Towards an understanding of the factors controlling bacterial diversity and activity in semi-passive Fe- and As-oxidizing bioreactors treating arsenic-rich acid mine drainage

Camila Diaz-Vanegas, Angélique Desoeuvre, Marina Héry, Odile Bruneel, Catherine Joulian, Jérôme Jacob, Fabienne Battaglia-Brunet, Corinne Casiot

OXFORD UNIVERSITY PRESS | FEMS Microbiology Ecology

http://mc.manuscriptcentral.com/fems

Towards an understanding of the factors controlling bacterial diversity and activity in semi-passive Fe- and As-oxidizing bioreactors treating arsenic-rich acid mine drainage

Journal:	*FEMS Microbiology Ecology*
Manuscript ID	FEMSEC-23-02-0064.R1
Manuscript Type:	Research article
Date Submitted by the Author:	12-Jul-2023
Complete List of Authors:	Diaz-Vanegas, Camila; HydroSciences Montpellier, University of Montpellier, CNRS, IRD, Montpellier, France hery, marina; HydroSciences Montpellier, University of Montpellier, CNRS, IRD, Montpellier, France Desoeuvre, Angélique; HydroSciences Montpellier, University of Montpellier, CNRS, IRD, Montpellier, France Bruneel, Odile; HydroSciences Montpellier, University of Montpellier, CNRS, IRD, Montpellier, France Joulian, Catherine; BRGM, Environnement et Procédés Jacob, Jérôme; BRGM, DEPA Battaglia-Brunet, Fabienne ; BRGM, DEPA Casiot-Marouani, Corinne; HydroSciences Montpellier, University of Montpellier, CNRS, IRD, Montpellier, France
Keywords:	acid mine water, microbial ecotoxicology, biological arsenic oxidation, biological iron oxidation, bioremediation, aioA gene

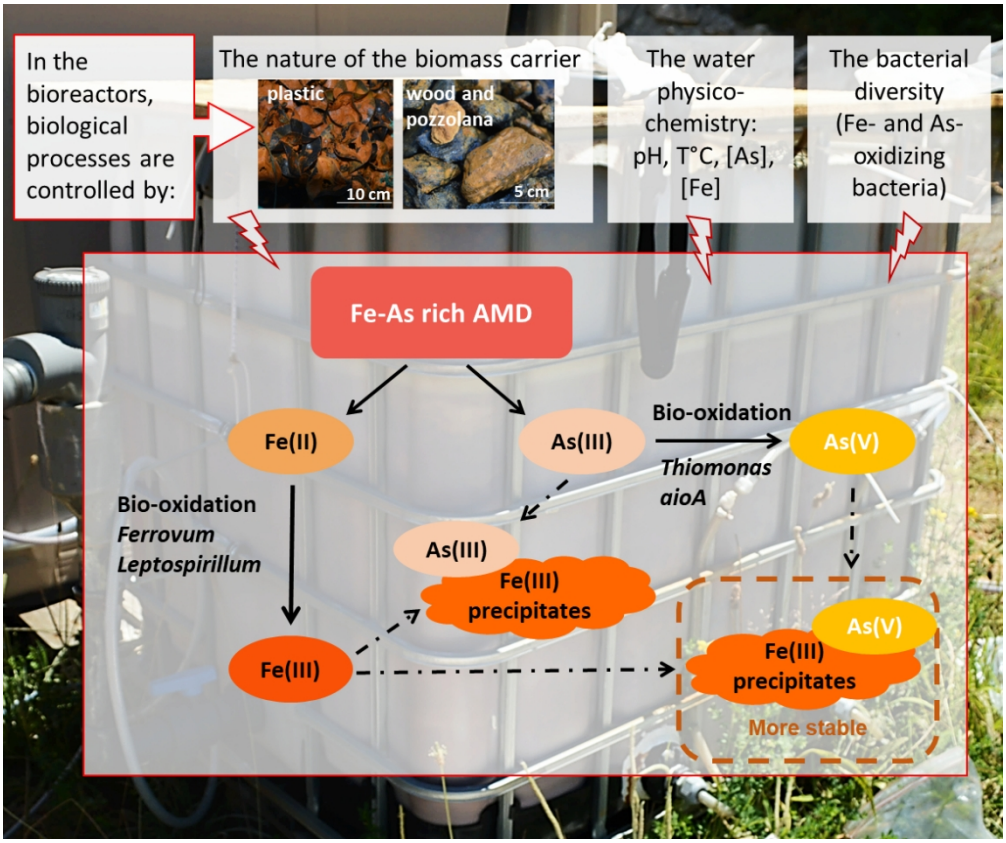

501x418mm (59 x 59 DPI)

Towards an understanding of the factors controlling bacterial diversity and activity in semi-passive Fe- and As-oxidizing bioreactors treating arsenic-rich acid mine drainage

*Diaz-Vanegas C[1,2], Héry M[*1], Desoeuvre A[1], Bruneel O[1], Joulian C[2], Jacob J[2], Battaglia-Brunet F[2], Casiot C[1]*

[1] *HydroSciences Montpellier, Univ. Montpellier, CNRS, IRD, Montpellier, France*

[2] *French Geological Survey (BRGM), Water, Environment, Process and Analyses Division, Orléans, France*

**Corresponding author*

E-mail address: (Héry Marina) marina.hery@umontpellier.fr

Abstract

Semi-passive bioreactors based on iron and arsenic oxidation and co-precipitation are promising for the treatment of As-rich acid mine drainages. However, their performance in the field remains variable and unpredictable. Two bioreactors filled with distinct biomass carriers (plastic or a mix of wood and pozzolana) were monitored during one year. We characterized the dynamic of the bacterial communities in these bioreactors, and explored the influence of environmental and operational drivers on their diversity and activity. Bacterial diversity was analyzed by 16S rRNA gene metabarcoding. The *aioA* genes and transcripts were quantified by qPCR and RT-qPCR. Bacterial communities were dominated by several iron-oxidizing genera. Shifts in the communities were attributed to operational and physiochemical parameters including the nature of the biomass carrier, the water pH, temperature, arsenic and iron concentrations. The bioreactor filled with wood and pozzolana showed a better resilience to disturbances, related to a higher bacterial alpha diversity. We evidenced for the first time *aioA* expression in a treatment system, associated with the presence of active *Thiomonas* spp. This confirmed the contribution of biological arsenite oxidation to arsenic removal. The resilience and the functional redundancy of the communities developed in the bioreactors conferred robustness and stability to the treatment systems.

Keywords: acid mine water, microbial ecotoxicology, biological arsenic oxidation, biological iron oxidation, bioremediation, *aioA* gene

Introduction

Acid mine drainages (AMD) are undesired products of the weathering of sulfide minerals present in mining wastes. They contribute to decreasing the pH and releasing metals and metalloids into aquatic environments. Arsenic is associated with more than 200 minerals (Alam and Mcphedran, 2019) such as arsenopyrite (FeAsS). Their oxidation releases this toxic metalloid, which is mobilized across the aquatic bodies downstream of the mine tailings (Paikaray 2015). The chronic toxicity of arsenic is a threat to public and environmental health (Huq *et al*., 2020).

Closed and abandoned mines are the main source of AMD (Rezaie and Anderson 2020). Because the cost of remediation is often covered by limited public funds, the development of cost-effective and low-maintenance treatments is necessary. Autochthonous microbial communities thriving in AMD containing arsenic are the key to treat this pollution. Indeed, bacterially mediated iron (Fe) and arsenic (As) oxidation, followed by their co-precipitation is a natural process responsible for the partial removal of the arsenic present in AMD (Casiot *et al.,* 2003; Asta *et al.,* 2010). Arsenic is usually present in AMD under the arsenite As(III) form. Biological oxidation of As(III) to As(V) contributes to reduce its mobility, due to the higher affinity of As(V) with the Fe-rich solid particles present in mine wastes and streams (Maillot *et al.,* 2013). Thus, the combined action of Fe- and As-oxidizing bacteria contributes to arsenic and iron removal from polluted waters.

The Reigous creek, near the former Carnoulès mine (Southern France), is an exceptional example of an arsenic impacted AMD that has been extensively studied during more than 20 years (Leblanc *et al.,* 1996, 2002; Casiot *et al.,* 2003; Egal *et al.,* 2010; Volant *et al.,* 2014). Seasonal variations of the physico-chemistry of the AMD waters were evidenced (Egal *et al.,* 2010) and were associated with temporal dynamics of the bacterial diversity (Volant *et al.,* 2014). On site, natural attenuation mediated by Fe(II)- and As(III)-oxidizing bacteria is responsible for the removal of about 30% of the soluble As in the first 40 m of the creek, through the formation of biogenic precipitates such as tooleite, schwertmannite and

amorphous As(V)- and As(III)-Fe(III) phases (Casiot *et al.,* 2003*;* Morin *et al.,* 2003; Egal *et al.,* 2010). However, natural attenuation is not sufficient to reach the water quality objective (0.83 µg L^{-1} over the local geochemical background value) set by European Water Directive (2000/60/EC) for dissolved As concentration in freshwater. Furthermore, the accumulation of As-rich biogenic precipitates in the creek bed is of concern due to the possible remobilization of As during extreme rainfall events affecting the region (Resongles *et al.,* 2014, 2015).

Previous studies have attempted to develop a treatment system for As-rich AMD based on natural attenuation process (Hedrich and Johnson, 2012; Macías *et al.,* 2012; Ahoranta *et al.,* 2016; Fernandez-Rojo *et al*., 2017, 2018, 2019). Fernandez-Rojo *et al.,* (2017, 2018) obtained nearly 80% As removal in a laboratory-scale continuous flow bioreactor, fed with the Carnoulès AMD. Later, a first attempt made with an *in situ* pilot suffered important performance variations and highlighted the importance to optimize oxygenation and support for bacterial attachment (Fernandez-Rojo *et al.,* 2019). The dynamic of the bacterial communities inside this field pilot was described by Laroche *et al.,* (2018). Arsenate (As(V)) enrichment in the biogenic precipitates was associated with an increase in the abundance of As(III)-oxidizing bacteria. However, to the best of our knowledge, the expression of the As(III) oxidase, which catalyzes a key process in such treatment, has not been evidenced yet in a treatment system. Only the genetic potential for As(III) oxidation has been revealed by the detection of the *aioA* gene (Fernandez-Rojo *et al*., 2017; 2019). Furthermore, there are still gaps to be filled about the stability of the bacterial diversity and activity facing seasonal and operational fluctuations, and the implications on treatment efficiency and robustness (Fernandez-Rojo *et al.,* 2019). Recently, we obtained a relatively stable As removal efficiency (67%) in two optimized semi-passive field bioreactors using air injection and biomass carriers. These semi-passive treatment units, monitored during one year, showed improved and more stable performances compared to previous field study and are promising for the treatment of arsenic-rich AMD. Understanding the dynamic of the bacterial communities in such systems is of prime importance since Fe oxidation only relies on bacterial activity at acid pH and As oxidation is bacterially catalyzed.

Hence, the present work aims to characterize the bacterial diversity and activity in the two optimized semi-passive field bioreactors described by Diaz-Vanegas *et al.*, (2022) under varying on-site operating and seasonal conditions. Two types of biomass carriers (plastic support and a mix of wood chips and pozzolana) were compared. We focused on active

bacterial communities through the analysis of environmental RNA and distinguished the communities attached to the supports to those in suspension. Bacterial diversity was determined by metabarcoding of the 16S rRNA gene and the presence and the expression of the As(III) oxidase gene quantified by quantitative PCR (qPCR). Then, we related the microbiological parameters to bioreactors performances and discussed the links between the dynamic of the bacterial communities, the variations of the physico-chemistry of the AMD water and the system treatment stability.

Materials and methods

Bioreactor setup, operation and sampling

Two bioreactors of 1 m^3 each were installed downstream the Carnoulès tailing dam as described in Diaz-Vanegas *et al.,* (2022). Briefly, the bioreactors were continuously fed with the Carnoulès' AMD and the flow rate was controlled by pumps. Each bioreactor was equipped with air diffusers to avoid oxygen limitation. One bioreactor was filled with a plastic biomass carrier ("PS") (Biofill, Type A), the other with a mixture of coarse wood chips and pozzolana ("WP" for Wood-Pozzolana). The two biomass carriers showed different properties: the plastic carrier reactor had higher porosity (96%) but lower specific surface area (>160 m^2 m^{-3}) than the wood-pozzolana mixture (porosity: 64% and specific surface area estimated to 333 m^2 m^{-3}).

The bioreactors were monitored during 218 days. Monitoring covered all seasons and was divided in seven periods A, B, C, D, E, F and G from July 2019 to September 2020. The periods were defined based on the flow rate and some undesired interruptions due to technical and operational issues and sanitary crisis. Water circulation was stopped between period A and B due to an electrical supply problem (September-November), so during three months the bioreactors were operated in batch conditions. During period F and beginning of period G, the accumulation of biogenic precipitates led to clogging of the air diffusers in both bioreactors. The air diffusers started working properly again after a maintenance later in period G (September), 15 days before the last sampling.

Occasional sampling of the inlet water (i.e. the AMD water feeding the two bioreactors) was carried out once during period B (19th of December 2019) and once during period F (27th of July 2020). Outlet waters and biogenic precipitates formed inside the reactors were collected

periodically for bacterial community characterization. Sample collection began in period B (due to the time required to form sufficient quantity of precipitates), and was carried out once per period for each bioreactor.

The attached communities correspond to the bacterial communities living in the biogenic precipitates accumulated in the biomass carriers. These biogenic precipitates were collected by scrapping the biomass carrier in each bioreactor. In the WP bioreactor, they were sampled only from the wood chips (due to the difficult access to the pozzolana at the bottom of the tank). Samples were collected in Falcon tubes (50 mL) and left some minutes for decantation. The supernatant was discarded and the precipitates were distributed into six cryo-tubes (2 mL). The suspended communities correspond to the bacteria living in the aqueous phase and associated with the suspended particulate matter (SPM) recovered from filters (0.22 µm). For each point of water sampling (outlet PS,outlet WP, and inlet water), six replicates of outlet water (300 mL each one) were filtered on sterile 0.22 µm cellulose acetate filters.
All the solid samples and filters were flash-frozen in dry ice in the field, transported to the laboratory and stored at -80 °C until DNA and RNA extractions.

Geochemistry of the waters and the biogenic precipitates and performance of the two bioreactors

The chemical characterization of the inlet water, outlet water and biogenic precipitates of each bioreactor is detailed in our previous study (Diaz-Vanegas *et al.,* 2022). The data for inlet and outlet waters corresponding to the sampling performed for microbiological analyses are summarized in Table 1 and Table SI 1. These data were used for the correlation analyses. In the inlet water, As concentration varied between 50 and 100 mg L^{-1} and Fe concentration between 500 and 1000 mg L^{-1}. The AMD was more concentrated in pollutants during the driest and hottest seasons (periods E, F and G) as described before (Egal *et al.,* 2010). The pH of the AMD varied between 3.7 and 4.8, with the highest values during period B. The AMD showed a temperature between 8 and 22°C with the highest value during period E. The coldest temperature was measured during periods B and C, which also correspond to the periods with the lowest concentration of total Fe (449-501 mg L^{-1}) and As (49-54 mg L^{-1}). The hydraulic retention time (HRT) was slightly different between the two devices, with approximately one hour more in the WP device. Two HRT were tested (~ 9h and ~ 18h), but the difference in the performances (rates of Fe and As oxidation and precipitation) was less

than 10%. Occasional measurements of dissolved oxygen concentration inside the bioreactors showed dysfunction of the air diffusers in period F.

Both bioreactors showed similar Fe oxidation and As removal rates, represented respectively by the first-order kinetic constant of Fe oxidation KOFe and the As precipitation rate determined in Diaz-Vanegas *et al.,* (2022). The highest performances were obtained during period E (Fe oxidation) and F (As precipitation) as shown in Figure 1. In the biogenic precipitates, more than 60 % of total As was under the As(V) oxidation state during the entire monitoring (Table SI 2).

The performance indicators used for the correlations include the KOFe (min^{-1}), Fe precipitation rate (mol $L^{-1}s^{-1}$), As precipitation rate (mol $L^{-1}s^{-1}$) and percentage of As(V) released in the outlet water (As(V)% outlet).

Environmental DNA and RNA extraction and cDNA synthesis

The molecular characterization of the total and active bacterial communities was based on the analyses of environmental DNA and RNA (cDNA) respectively. For each bioreactor, DNA was extracted from biogenic precipitates and water filters using DNeasy PowerSoil kit and DNeasy PowerWater kit (Qiagen) respectively, according to the manufacturer's recommendations. The RNA extractions were performed from biogenic precipitates and outlet water filters using FastRNA Pro Soil-Direct kit (MP Biomedicals) and RNeasy Power Water Kit (Qiagen) respectively, according to the manufacturer's recommendations. Residual DNA was removed from the extracted RNA with an additional Turbo DNase treatment (Turbo DNA-free kit, Ambion). The absence of DNA was confirmed by the absence of amplification, from RNA extracts, of 16S rRNA gene with 8F (5′-AGAGTTTGATCCTGGCTCAG-3′, Lane 1991) and 1489R (5′-TACCTTGT TACGACTTCA-3′, Weisburg *et al.,* 1991) primers. Reverse transcription was immediately performed on DNA-free RNA extracts using the iScript™ cDNA Synthesis Kit (Biorad).

The quality of the cDNA was confirmed by performing a PCR targeting 16S rRNA gene using 8F and 1489R primers or *aioA* gene using aoxBM1-2F (5-CCACTTCTGCATCGTGGGNTGGGNT A-3) and aoxBM3-2R (5-TGTCGTTGCCCCAGATGADNCCYTTYT-3) primers (degenerate primers designed to target mutliple bacterial and archaeal taxa, Quéméneur *et al.,* 2008). DNA and RNA extracts

were quantified with a fluorometer (Qubit ®, Invitrogen) and stored at -80°C until further analysis.

Sequencing of 16S rRNA gene and bioinformatics

For metabarcoding, the V3-V4 region of the bacterial 16S rRNA gene was targeted using primers 341F (5'-CCTACGGGNGGCWGCAG-3') and 805R (5'-GACTACHVGGGTATCTAATCC-3'). Libraries of amplicons and Illumina MiSeq sequencing were performed by MetaHealth metagenomic-based services (CIRAD, PHIM, Eco&Sols, Montpellier, France) for biogenic precipitates and outlet waters.

Illumina sequencing, base calling and demultiplexing were carried out using RTA v1.18.54, MCS 2.6 and bcl2fastq 2.17. Paired Illumina MiSeq reads were assembled with vsearch v2.18.0 (Rognes *et al.,* 2016) using the command fastq_mergepairs and the option fastq_allowmergestagger. Demultiplexing and primer clipping were performed with cutadapt v3.4 (Martin 2013) forcing a full-length match for sample tags and allowing a 2/3-length partial match for forward and reverse primers. Only reads containing both primers were retained. For each trimmed read, the expected error was estimated with vsearch's command fastq_filter and the option eeout. Each sample was then dereplicated, i.e. strictly identical reads were merged, using vsearch's command derep_fulllength, and converted to FASTA format.

To prepare for clustering, the samples were pooled and processed by another round of dereplication with vsearch. Files containing expected error estimates were also dereplicated to retain only the lowest expected error for each unique sequence. Clustering was performed with swarm v3.1.0 (Mahé *et al.,* 2021), using a local threshold of one difference and the fastidious option. Operational taxonomic unit (OTU) representative sequences were then searched for chimeras with vsearch's command uchime_denovo (Edgar *et al.,* 2011). In parallel, representative sequences were assigned using the stampa pipeline (https://github.com/frederic-mahe/stampa/) and a trimmed version of the reference database SILVA SSURef NR99 v138.1 (Quast *et al.,* 2013).

Clustering results, expected error values, taxonomic assignments and chimera detection results were used to build a raw OTU table. Up to that point, reads that could not be merged, reads without tags or primers, reads shorter than 32 nucleotides and reads with uncalled bases ("N") had been eliminated. To create the "cleaned" OTU table, additional filters were applied

to keep only non-chimeric OTUs, OTUs with an expected error per nucleotide below 0.0002, OTUs containing more than three reads or seen in at least two samples. The raw data are available under the bioproject (https://www.ebi.ac.uk/ena/data/view/PRJEB63466).

The OTU table was processed with R 3.5.2 (R Core Team, 2018) for additional filtering steps and statistical analysis with the packages tidyverse 1.3.0 (Wickham 2017) and vegan 2.5.6 (Oksanen *et al.,* 2018). These steps include removing the controls and the samples with less than 1000 reads, and the rarefaction of the remaining samples.

aioA and 16S rRNA genes and transcripts quantification

Abundance of the *aioA* gene (encoding the catalytic subunit of the arsenite oxidase) and of the bacterial 16S rRNA genes and their transcripts were quantified by a real-time quantitative PCR (qPCR) from the DNA extracts and from the cDNA, respectively. For 16S, we used universal primers 341F (5'CCTACGGGAGGCAGCAG-3') and 515R (5'ATTACCGCGGCTGCTGGCA-3'). For *aioA*, we used primers m4-1F (5'GCCGGCGGGGGNTWYGARRAYA-3') and m2-1R (5'GGAGTTGTAGGCGGGCCK RTTRTGDAT-3) (degenerate primers designed to target multiple bacterial and archaeal taxa, Quéméneur 2008). The qPCR was performed with the CFX Real-Time PCR Detection system (Bio-Rad), using SSO Advanced SYBR® Green Supermix and each primer at 0.4 µM (16S rRNA gene) or 0.3 µM (*aioA* gene). Calculation of copy numbers was done using a linear calibration curve ($r^2 > 0.9$) obtained over 7 orders of magnitude, ranging from 10^2 to 10^8 gene copies of a linearized plasmid carrying the target gene (gene copies/mL of water or mg of biogenic precipitates).

Biostatistical analysis

All statistical analyses were performed with R version 3. Chao1 and Shannon indices were calculated using the vegan and ggplot2 packages for biological diversity statistics in R (Wickham 2017; Oksanen *et al.,* 2018). Bray Curtis was used as diversity metric to compare the bacterial communities from each bioreactor (R packages phyloseq and dplyr (McMurdie and Holmes 2013; Wickham *et al.,* 2022).

The analysis of similarity (ANOSYM, 999 permutations) was performed to compare the statistical differences between pre-defined groups. It allowed us to compare the results obtained for the structure of the bacterial communities based on the following criteria:

biomass carrier WP versus PS, the different periods of monitoring, the total (DNA) versus the active (RNA) communities, and the suspended versus the attached bacterial communities (R package vegan, Oksanen *et al.,* 2018).

A non-metric multidimensional scaling (NMDS) ordination was used to visualize bacterial community variations among samples, the differences among the structure of the communities are represented by the distance between the points. The Indicators Species Analysis was performed to identify the main species responsible for the differences in bacterial community composition between defined groups (R package indicspecies, De Caceres and Legendre, 2009).

Significant differences between the different groups were detected with one-way ANOVA (p-value 0.05) followed by Tukey test. The data that did not follow a normal distribution were analyzed by Kruskal-Wallis test. Finally, the correlations between biological and physicochemical variables were performed by the Spearman test, Spearman was used instead of Pearson's correlation due to non-normal distribution of the data (R package heatmaply, Galili *et al.,* 2017).

Results

General description of the bacterial diversity

Illumina sequencing yielded a total of 5 119 340 sequences of bacterial 16S rRNA gene corresponding to 116 samples. Considering all periods together, based on Chao 1 (richness) and Shannon (evenness and richness) indices, the alpha diversity was higher (Kruskal-Wallis, p-value < 0.001) in the bioreactor filled with the wood and pozzolana (WP) than in the bioreactor with the plastic carrier (PS) (Figure 2.a). For both bioreactors, the richness (Chao1) of the suspended community sampled from the outlet water was higher than the one of the attached communities sampled from the biogenic precipitates (Kruskal-Wallis, p-value < 0.05), but the Shannon index (which takes into account evenness) followed the opposite trend (p-value < 0.01) (Figure SI 1.a). Alpha diversity indices measured for the overall active and total bacterial communities were similar (Figure SI 2.a; Kruskal-Wallis, p-value > 0.05).

The results obtained for the beta diversity (reflecting the taxa turnover) did not follow the same trend as the one obtained for the alpha diversity. Indeed, we observed a higher beta diversity associated with the PS bioreactor compared to the WP bioreactor (Mann-Whitney;

p-value <0.0001) (Figure 2.b). Also, the suspended community showed higher beta diversity than the attached communities (Figure SI 1.b; Mann-Whitney; p-value <0.0001). Finally, the total bacterial community presented higher beta diversity than the active one (Figure SI 2.b; Mann-Whitney; p-value <0.0001).

Dynamic of the bacterial community structures in the PS and WP bioreactors

The dynamic of the bacterial communities developed in both bioreactors was represented by non-metric multidimensional scaling (NMDS) (Figure 3). In complement, an ANOSIM test was used to determine significant differences in the bacterial community composition of groups of samples. Groups were defined according to the sampling period, the nature of the biomass carrier, the lifestyle (attached versus suspended communities) and the metabolic status (total versus active communities). The most important differences were observed between the different periods of monitoring (represented by the different colors in the NMDS) (ANOSIM test, R 0.4463, p-value = 0.001). There were marked variations in the bacterial community structure particularly between the first periods of monitoring (B and C), and the next ones (D, E, F and G). These variations were more pronounced for the PS bioreactor than for the WP, reflected by the wider ellipse shown in Figure 3, and in agreement with the higher beta diversity measured in PS (Figure 2.b).

The influence of both lifestyle and biomass carrier was moderate compared to the temporal dynamic (ANOSIM test, R 0.4463, p-value = 0.001). The lifestyle (suspended or attached in the biogenic precipitates) was the second criteria driving the bacterial communities (ANOSIM test, R 0.1935, p-value = 0.001) and the third criteria was the biomass carrier (plastic or wood/pozzolana) (ANOSIM test, R 0.1535, p-value = 0.001). Finally, active communities were relatively distinct from the total ones during the first stage of the monitoring (period B and C). During the other periods, the structure of the active and the total communities appeared more similar. Overall, the status (total versus metabolically active) of the bacterial communities was the factor explaining the less the differences between the samples (ANOSIM test, R 0.05191, p-value = 0.002).

Indicators species analysis revealed the bacterial taxa that contributed the most to the shifts in the bacterial communities. For instance, *Gallionella* and *Gallionellaceae*-related sequences dominated the PS bioreactor during periods B and C. *Acidicapsa*, *Acidiphium*, *Acidibacter*,

Acidibrevibacterium, *Granulicella* and *Tepidsphareales*-related sequences were representative of samples collected in the WP bioreactor particularly during the first periods B and C. *Acidithiobacillus* was representative of samples collected in the PS bioreactor at the end of the monitoring (periods F and G). *Thiomonas* was representative of the total and the metabolically active bacterial communities in both bioreactors particularly during period E.

Taxonomic composition of the bacterial communities thriving in the two bioreactors

The most abundant phyla identified in the outlet waters and the biogenic precipitates sampled in both bioreactors were *Proteobacteria* (62%) and *Nitrospirota* (35%). *Acidobacteria* was the third more abundant phylum, representing only 1% of the total number of sequences. On the whole data set, the dominant genera were the iron-oxidizing (FeOB) bacteria *Leptospirillum*, *Ferrovum, Acidithiobacillus* and an undetermined genus of the *Gallionellaceae* family. *Leptospirillum* was abundant and active from the beginning to the end of the monitoring, mainly in the biogenic precipitates. *Ferrovum* was more abundant and active in the suspended community (outlet water), particularly during the D period of the monitoring.

The dynamic of the FeOB populations was different in the two bioreactors (Figure 4). In the PS bioreactor, the first two periods B and C (December and February) were dominated by *Leptospirillum*, *Gallionella*, and an undetermined genus from *Gallionellaceae* family, while in the WP bioreactor, *Leptospirillum* was the only dominant FeOB. Then, the FeOB populations evolved towards a dominance of *Ferrovum* and *Leptospirillum* in both bioreactors. At the end of the monitoring (period F and G), the communities of the PS bioreactor were enriched with *Acidithiobacillus. Gallionella* was mainly present and active during the first stage of the monitoring only in the suspended community of the WP bioreactor, but present in both suspended and attached communities in the PS bioreactor.
The OTUs affiliated to the *Gallionellaceae* family were dominant in PS bioreactor in the suspended and attached communities during period B and C, but they relative abundance dramatically decreased from period D. In a lesser extent, the same trend was observed for *Acidocella* and *Granulicella*.

Thiomonas was the sixth most dominant genus identified in the metabarcoding data (Figure 4). It was always detected in both the total and active communities, although its distribution showed a different pattern in the two bioreactors. In the WP bioreactor, *Thiomonas* was more abundant in the suspended community during period E, with a similar trend between total and active communities. On the contrary, in the PS bioreactor, *Thiomonas* was more represented in the attached community, with a stable abundance over time. *Acidiphilium* was present in both bioreactors, for most of the monitoring period, but was more represented in the attached community than in the suspended community. *Metallibacterium* was present in relatively low proportions in both systems, and RNA-based analysis showed that this genus was probably not metabolically active.

Indicator Species Analysis supported our previous observations about the bacterial genera representative of a particular group; in the attached communities (biogenic precipitates) the representative genera were *Acidiphilium, Leptospirillum, Acidibacter, Acidicapsa* for both bioreactors, and *Acidocella, Acidibrevibacterium* and *Granulicella* for WP only. On the contrary, *Ferrovum* and *Sideroxydans* were representative of the suspended community in both bioreactors. *Legionella* and an undetermined genus of *Acidobacteriaceae* family were representative of the suspended community only in the WP bioreactor.

Abundance and expression of 16S rRNA and aioA genes

Based on environmental DNA analysis, the 16S rRNA gene copy number varied between 10^2 and 10^6 copies mg^{-1} of biogenic precipitate and between 10^4 to 10^7 copies mL^{-1} of water in both bioreactors (Figure 5.a and 5.b). The average bacterial biomass of the biogenic precipitates community was similar in the two bioreactors (Figure 5.a). The average biomass of suspended communities in water remained stable between the inlet and the outlet water of the PS and WP bioreactors (Figure 5.b). The biomass varied over time without any clear trend (Figure SI 3).

Results based on cDNA showed between 10^3 to 10^6 16S rRNA transcripts mg^{-1} of biogenic precipitate and between 10^3 to 10^5 16S rRNA transcripts mL^{-1} of outlet water, without difference between the two bioreactors (Figure 5.a and 5.b).

Based on DNA analysis, the number of *aioA* genes in both bioreactors varied between 10^1 and 10^5 copies mg^{-1} of biogenic precipitate and between 10^2 and 10^6 copies mL^{-1} of water (Fig 5.c and 5.d). The number of genes and the number of transcripts of the arsenite oxidase were similar in both bioreactors (Figure 5.c and 5.d), except for the attached community of WP in which *aioA* transcripts remained below the detection limit (Figure 5.c). The expression of the arsenite oxidase gene was evidenced (by detection of *aioA* transcripts) in 14 of a total of 60 samples, and showed up to 150 transcripts mL^{-1} of water in the WP bioreactor during period E and up to 421 transcripts copies mg^{-1} of biogenic precipitate in the PS bioreactor in period C (Figure SI 3). In the other samples, recovery of *aioA* transcripts was below the detection limit. The results suggest that the As(III)-oxidizing activity might be more expressed during period E and C, compared to other periods. However, technical limitations associated with mRNA extraction yield and cDNA synthesis could have interfered with the analysis.

For DNA-based analyses, the relative abundance of bacteria carrying *aioA* gene in the bacterial community and its dynamic in the bioreactors were assessed based on *aioA*/16S rRNA genes ratio (Figure 6). In the WP bioreactor, the suspended bacterial communities sampled at period E was the most enriched in As(III)-oxidizing bacteria (0.6 copies of *aioA*/16S rRNA ratio). On the contrary, in the PS bioreactor, the attached communities were the most enriched in As(III)-oxidizing bacteria. The highest enrichment was observed for periods C, D and E (average of 0.35 copies of *aioA*/16S rRNA ratio).

The relative abundance of *aioA* gene varied widely according to the period, the bioreactor and the lifestyle, but without any clear trend. For instance, the average of the relative abundances of arsenite oxidase gene was similar in the outlet waters of both bioreactors (0.09 ± 0.15 copies of *aioA*/16S rRNA ratio) and the feed water (Carnoulès AMD) (0.07 ± 0.02 copies of *aioA*/16S rRNA ratio, data not shown).

Links between the bacterial communities and the physicochemical characteristics of the AMD or the treatment performances.

Correlations between the microbiology (abundance of the 13 most dominant bacterial taxa developed in the bioreactors) and the physico-chemistry of the AMD were assessed by calculating Spearman's coefficients (significant when the coefficient was ≥ 0.5 or ≤ -0.5). Correlations were also determined between the microbiology and the variables reflecting the performance of the treatment system (kinetic constant value KOFe, Fe precipitation rate, As

precipitation rate, As(V) % in the outlet, pH outlet) or the operating condition (HRT) (Figure 7).

The relative abundance of sequences related to *Ferrovum*, *Acidithiobacillus* and *Acidobacteriaceae* were positively correlated with dissolved As concentration, temperature and Fe(II) concentration in the inlet water (correlation > 0.5). In a lesser extent, *Thiomonas* also showed a positive correlation with those parameters. On the contrary, taxa *Gallionella* and *Gallionellaceae*-undetermined genus showed a negative correlation with those parameters (correlation -0.5). The relative abundance of As(III)-oxidizing bacteria (*aioA*/16S rRNA ratio) was positively correlated with the temperature, the total dissolved As concentration and the percentage of As(III) in the inlet water. The rates of Fe precipitation and As precipitation were strongly positively correlated with the relative abundance of *Ferrovum* (correlation 0.6 and 0.7 respectively). The percentage of As(V) in the outlet water was positively correlated with the relative abundance of the As(III)-oxidizing genus *Thiomonas* (correlation 0.6) and in lesser extent with *Acidobacteraceae*-undetermined genus and *Acidiphilium* (correlation 0.5). On the contrary, this parameter was negatively correlated with *Gallionella* and *Gallionellaceae*-undetermined genus (correlation -0.5). The pH of the outlet water was positively correlated with the abundance of *Gallionella* and *Gallionellaceae*-undetermined genus (correlation 0.5) and negatively correlated with *Ferrovum* (correlation -0.7).

The relative abundance of the As(III)-oxidizing bacteria (*aioA*/16S rRNA genes ratio) was strongly positively correlated with *Thiomonas* (correlation 0.8). Two HRT were applied in both bioreactors (~9h and ~18h). There was a positive correlation between the relative abundance of *Acidibrevibacterium*, *Acidiphilium* and *Acidobacteriaceae* relative sequences and HRT. However, no significant correlation between the FeOB and the HRT was evidenced.

Discussion

Characterization of the total and active bacterial communities

Total and active bacterial communities were dominated by Fe-oxidizing bacteria (FeOB) (*Leptospirillum*, *Ferrovum*, *Acidiothiobacillus*, an undetermined genus of *Gallionellaceae*,

and *Gallionella*). *Ferrovum* was over-represented in the active community (37% and 21% in the whole RNA and DNA data sets respectively). This finding is in line with the probable important role played by this Fe-oxidizing bacteria in the treatment of the Carnoulès AMD, as reported in other studies (Heinzel *et al*., 2009; Sheng *et al.,* 2016; Wang *et al.,* 2016; Grettenberger *et al.,* 2020). *Leptospirillum* followed the same trend but in a lesser extent (38 and 36% respectively). On the contrary, *Acidithiobacillus*, undetermined genus of *Gallionellaceae* and *Gallionella* were more abundant in the total than in the active community, suggesting their possible limited contribution to the treatment process. In particular, *Acidithiobacillus* represented 9 % of the total DNA sequences and only 5 % of the cDNA sequences reinforcing the idea of its possible lower efficiency in remediation systems compared to other FeOB (Heinzel *et al.,* 2009; Laroche *et al.,* 2018). Ebrahimi *et al.,* (2005) observed that the short dominance of *Acidithiobacillus ferroxidans* was accompanied by a treatment efficiency limited to 90% while a shift towards *Leptospirillum* dominance probably contributed to an increase of the performances up to 98%.

Ferrovum was more represented in the suspended community than in the attached one. Its capacity to release extracellular polymeric substances (EPS) (Johnson *et al.,* 2014; Plewniak *et al.,* 2020) could promote its development in the small iron flocs suspended in the outlet water (Florence *et al.,* 2016). *Ferrovum* has been previously associated with “acid streamers”, which are macroscopic biofilms formed by acidophilic microorganisms (Hedrich and Johnson 2012; Kay *et al.,* 2013).

Thiomonas was the fourth most abundant genus active in both bioreactors (4% of the whole cDNA sequences and 2% of the whole DNA sequences). This genus was present in a similar abundance in a laboratory bioreactor treating the Carnoulès AMD (2% of DNA sequences, Fernandez-Rojo *et al.,* 2018). These proportions are higher (but of the same order of magnitude) as those found in the Regious Creek sediments (1.1% of DNA sequences, Laroche *et al.,* 2018).

Heterotrophic Fe(III)-reducing bacteria were also detected: genera *Acidiphillum* (3% and 2.5% of the total and the active community, respectively), *Acidibacter* (0.6 % of both communities), *Acidocella* (1.7% and 0.3% of the total and the active community, respectively), *Metallibacterium* (1.3 % and 0.3 % of the total and the active community, respectively). They were previously reported in acidic mine waters (Afzal Ghauri *et al.,* 2007; Johnson *et al.,* 2014; Gavrilov *et al.,* 2019; Li *et al.*, 2020) and in Fe-oxidizing bioreactors (Sheng *et al.,* 2016; Jin *et al.,* 2020). Most of these Fe(III)-reducing bacteria are characterized by a metabolic versatility including Fe(III) reduction, carbon fixation and sulfur oxidation

capacities (Hao *et al.*, 2010; Bartsch *et al.,* 2017; Gavrilov *et al.,* 2019; Li *et al.*, 2020). These bacteria were globally poorly represented in the active community. However, oxygenation should be carefully controlled to avoid suitable conditions for ferric iron reduction, which would contribute to As remobilization into the aqueous phase (Tufano and Fendorf, 2008). Arsenic remobilization has indeed been evidenced from river sediments impacted by the Carnoulès AMD during incubation under anoxic conditions (Héry *et al.,* 2014).

Influence of the biomass carrier on the bacterial diversity

Biomass carriers provide a physical support for bacterial growth, extend their survival rate, and enhance oxygen transfer (Tyagi *et al.,* 2011). Al-Amshawee *et al.,* (2021) reported that the biomass attached to the carriers can be up to 500 times more resistant than suspended bacteria to sudden changes. In a membrane bioreactor, the surface of a biomass carrier provided a diversified environment, promoting the growth of diverse types of microorganisms (Li *et al*., 2021). On the contrary, diversity was higher in suspended than in attached communities in a waste water treatment plant, possibly due to oxygen limitation inside the biofilm (Kwon *et al.,* 2010). As recently reported (Zhu et al., 2022), the type of biomass carrier can also influence the diversity and composition of the bacterial communities developing inside the bioreactors.

Bioprecipitates were sampled from the surface of the plastic carriers or from the wood ships (no sampling on pozzolana due to the difficult access to the pozzolana at the bottom of the tank). During the early-stage of the monitoring, bacterial community developed on the PS biomass carrier was dominated by chemoautotrophs (i.e. *Galionellla* and *Leptospirillum*), while the one associated with WP carrier was composed by both chemoauthotrophs (i.e. *Leptospirillum*, *Acidiphillum*) and chemoheterotrophs (i.e *Acidobacteriaceae*, *Acidocella*, *Acidiphillum*, *Acidicapsa*, *Acidibacter* and *Acidibrevibacterium*).

Our first assumption to explain these differences was that organic carbon provided by the wood chips could promote the development of heterotrophic bacteria. The wood chips are often used in bioreactors as biofilm support as well as a source of organic carbon or electron donors (Lopez-Ponnada *et al.,* 2017; Zhao *et al.,* 2019). This concurs with occasional measurements of total organic carbon in the biogenic precipitates, indicating a much higher concentrations in the WP (71 ± 47 g kg^{-1}) than in the PS (3 ± 0.7 g kg^{-1} (dry wt.). However,

the difference was minor in the treated waters (outlet water WP: 5 ± 2 mg L^{-1}; PS: 3 ± 1 mg L^{-1}). Thus, it cannot be excluded that the organic carbon from the WP carrier corresponded to refractory organic matter. Furthermore, no known cellulolytic bacteria were evidenced in the WP bioreactor. Consequently, the metabolic pathways involved in organic carbon cycling in the WP bioreactor would require further investigations. *Gallionella* produces a variety of exopolymers that could be an advantage for its attachment on the plastic biocarrier (Emerson *et al.,* 2013). Furthermore, the organic carbon rich environment provided by the wood chips may have inhibited the proliferation of *Gallionella*, in the WP bioreactor. According to Fleming *et al.,* (2014), *Gallionella* negatively co-occurred with high concentrations of organic carbon.

Our second assumption to explain the differences of bacterial communities thriving on the two types of biomass carriers is related to their surface properties (i.e shape, porosity, surface roughness). According to Pereira *et al.,* (2000) and Campos-Quevedo *et al.,* (2021), the surface roughness is the most important parameter for bacterial colonization, mainly because the surface irregularities promote initial colonization and protect microorganisms from detachment. Thus, crevices, cracks and grooves of the wood chips could allow more diverse micro-habitats and for consequence a higher alpha diversity in the WP bioreactor. Feng *et al.,* (2017) reported that higher alpha diversity can be associated with improved resilience to disturbances. This is in line with the better performance recovery of the WP bioreactor (in term of Fe oxidation and precipitation, and of As removal) after operational disturbances (interruptions, changes in the HRT and clogging of the air diffusers) (Diaz-Vanegas *et al.,* 2022). Finally, lower beta diversity in the WP bioreactor reflects lower variability and thus higher stability of bacterial communities.

Despite bacterial community composition differences observed during the early stages, WP and PS bioreactors showed similar performances for all the periods of the monitoring. Thus the bacterial groups that differ between the two supports may not play an important role in the process. In the next stages, both carriers were covered by the same mineral phases: jarosite, amorphous schwertmannite and amorphous ferric arsenate (Diaz-Vanegas *et al.,* 2022), which replaced the wood chips and plastic carriers as support for biomass attachment. Such replacement of biomass carrier by precipitated minerals was described by Ebrahimi *et al.,* (2005). Kinnunen and Puhakka (2004) and Wang and Zhou (2012) also showed the role of jarosite on the attachment of FeOB in a fluidized-bed reactor and its efficiency to maintain a

stable bacterial concentration that enhance iron oxidation and promote Fe(III) precipitation by acting as jarosite seed.

Arsenic oxidation

The role of *Thiomonas* spp. in As oxidation in Carnoulès ecosystem has been demonstrated (Bruneel *et al.,* 2003; Morin *et al.,* 2003). The activity of arsenite oxidase was evidenced *in situ* in the Reigous by a proteomic approach (Hovasse *et al.,* 2016). The detection of *Thiomonas* by CARD FISH and metabarcoding recently suggested that As(III) oxidation occurred in a pilot treating arsenic-rich AMD *in situ* and was probably mediated by *Thiomonas* (Laroche *et al.,* 2018). Here, we evidenced for the first time the expression of the arsenite oxidase gene (*aioA*) concomitant with the presence of metabolically active *Thiomonas* in a bioreactor. Furthermore, the relative abundances of *aioA* genes and *Thiomonas*-related 16S rRNA sequences (Figure 6) were positively correlated. These result confirmed the contribution of As(III) oxidation mediated by *Thiomonas* spp. to the treatment process.

The detection of *aioA* gene in all the biogenic precipitates and the outlet waters confirmed the stable presence of As(III)-oxidizing bacteria in both bioreactors as observed in a previous field pilot (Laroche *et al.,* 2018). The relative abundance of As(III)-oxidizing bacteria strongly varied depending on the nature of the samples and the period, with a particular enrichment in the suspended community of the WP bioreactor during period E (56 ± 11%) and in the PS bioreactor during period C, D and E (12-34%). Thus As(III)-oxidizing bacteria may represent higher proportions of the total community compared to what was described in other systems. For instance, the relative abundance of *aioA* in geothermal samples ranged from 0.1 to 19.5% (Sonthiphand *et al.,* 2021). In groundwater systems of an old tin mine (containing a maximum of 10 µg L^{-1} Arsenic), the relative abundance of *aioA* gene ranged from 0.85 to 37.13% (Sonthiphand *et al.,* 2021). In the present study, high arsenic concentrations (50 to 100 mg L^{-1}) mainly in the As(III) form might explain the elevated concentration of As(III)-oxidizing populations quantified in the Carnoulès AMD (inlet water) that fed the PS and WP bioreactors. The conditions inside the bioreactors did not lead to a clear increase in As(III)-oxidizing bacteria abundance inside the treatment units compared to the density measured in the AMD (Figure 5.d).

The highest abundances of *aioA* genes and *aioA* transcripts, observed during period E, were concomitant with an increase of *Thiomonas*-related sequences. Period E was characterized by an increase of temperature by more than 5°C, an increase of the total Fe concentration (~ 100 mg L^{-1}), and total As concentration (~ 15 mg L^{-1}) (Table 1 and Diaz-Vanegas *et al.,* 2022). Similarly, Tardy *et al.,* (2018) showed, in batch experiment, that high temperature stimulated As(III) oxidation associated with an increase of both the abundance of *aioA* genes and of *Thiomonas* spp. Quéméneur *et al.,* (2010) found high *aioA* gene densities associated with high concentration of As in surface water.

As(III)-oxidizing bacteria distribution was different in the two bioreactors: they were more represented in the attached community in the PS bioreactor, and in the suspended one in the WP bioreactor. In opposition to the common idea that the formation of a carrier-attached biofilm enhances bacterial activity, Michel *et al.,* (2007) showed that As(III) oxidation activity of some *Thiomonas* strains was higher for the suspended cells than for the attached ones. This is in agreement with our results for the WP bioreactor, but contradictory with the results for the PS bioreactor. Consequently, in the present study, As(III) oxidation by *Thiomonas* did not seem to be conditioned by their lifestyle. It is also possible that the *Thiomonas* strains developed in the PS and WP bioreactors were able to switch from attached to suspended mode as reported by Farasin *et al.,* (2017). There is growing evidence that environmental bacteria are capable of alternating between the free living and the attached fractions (Grossart, 2010) and that the two fractions are connected (Tang et al., 2017).

Arsenic oxidation led to the enrichment into As(V) in the biogenic precipitates (80 ± 11 %) and in the outlet water (41 ± 26 %, compared with 25 ± 5 % in the inlet water) (Diaz-Vanegas *et al.,* 2022). Because of the higher affinity of As(V) for iron minerals (Paikaray 2015), As removal under its oxidized form is more efficient and stable.

Geochemical and environmental factors influencing bacterial diversity and activity

In AMD affected environments, bacterial diversity is under the control of geochemical and environmental parameters (Méndez-García *et al.,* 2014, 2015; Volant *et al.,* 2014). As supported by Spearman correlations, pH, dissolved Fe(II) and As concentrations as well as water temperature were drivers determining the dynamic of FeOB and As(III) oxidizers

populations in the bioreactors. pH has a strong direct and indirect influence on AMD microbial communities due to its relationships with geochemical variables such as minerals solubility. In particular, pH controls dissolved As and Fe concentrations in the AMD (Jones *et al.,* 2015; Méndez-García *et al.,* 2015).

In the present study, *Gallionella* and *Gallionellaceae*-related sequences showed a positive correlation with pH of both inlet and outlet waters. The decrease of their relative abundance in the PS bioreactor coincided with the decrease of the pH. From period D, the bacterial communities inside the bioreactors were enriched with *Ferrovum*, known for its capacity to grow in more acidic conditions than *Gallionella* (Ziegler *et al.,* 2013). Accordingly, *Ferrovum* showed a negative correlation with pH. All these findings are consistent with previous studies showing that *Gallionella* is favored at pH > 3 while *Ferrovum* are favored at pH < 3 (Jones *et al.,* 2015; Sheng *et al.,* 2017).

In AMD, dissolved ferrous iron (Fe(II)) is one of the main energy source for bacteria; thus, its concentration may be another important factor determining geochemical niches of FeOB (Jones *et al.,* 2015). Here, the relative abundance of *Gallionella* and *Gallionellaceae*-related sequences were negatively correlated with Fe(II) concentration as described elsewhere (Fleming *et al.,* 2014). The abundance of *Ferrovum* increased during period D and E in both bioreactors concomitantly to the increase of the Fe(II) concentration in the inlet water. Assignment of *Ferrovum* to high Fe concentration was also reported by Jones et al 2015.

In the PS bioreactor, *Acidithiobacillus* abundance increased when the highest Fe(II) concentrations (712-1049 mg L^{-1}) were measured in the inlet water (periods F and G). This is in contradiction with other study (Jones *et al.,* 2015) where this genus was restricted to lower Fe(II) concentration (< 224 mg L^{-1}). Then, another factor should be responsible for the dynamic of *Acidithiobacillus* in the PS bioreactor at the end of the monitoring. During periods F and G, oxygen limitation, due to the clogging of the aeration system, could be detrimental to *Ferrovum* and *Leptospirillum* (Ziegler *et al.,* 2013; Johnson *et al.,* 2014). Conversely, the capacity of *Acidithiobacillus* to live in microaerophilic conditions has been widely described (Dave *et al.,* 2008). Thus, the dynamic of *Acidithiobacillus* in the bioreactors may be attributed to the synergy of the lack of oxygenation, the different biomass carrier used or another undetermined factor.

Additional parameters that influence bacterial diversity in the bioreactors were dissolved As concentration and water temperature, as reported by Laroche *et al.,* (2018) and Tardy *et al.,* (2018). As discussed previously, the present study supports the positive influence of temperature on the raise of the relative abundance of *Thiomonas* / arsenite-oxidizing bacterial populations. In contrast, *Gallionella* and *Gallionellaceae*-related sequences were negatively correlated with As concentration and temperature of the inlet water, as observed by Fleming *et al.,* (2014). The positive correlations between *Ferrovum* abundance and temperature and arsenic concentration in the inlet water (Figure 7), have not been described before. They revealed the adaptation of *Ferrovum* to high As concentrations, which makes it a good candidate for the bioremediation of highly As-rich effluents. On the contrary, the negative correlation of *Gallionella* and *Gallionellaceae*-related sequences with As concentration, suggest their possible poor adaptability for the treatment of As rich AMD.

Links between treatment performance and microbiology

The integrated analysis of performance indicators (As and Fe precipitation rates and Fe(II) oxidation kinetic constant KOFe) and microbiological variables provides new insights about the relationships between total and active bacterial diversity and treatment efficiency during periods of optimal operation (B-E). The abundance of total and active *Leptospirillum* and *Ferrovum* were positively correlated with performance indicators. Both genera are well known for their highly efficient Fe-oxidation activity (Chen *et al.,* 2013; Johnson *et al.,* 2014). The maintenance of their activity even at high As concentration (50 – 100 mg L^{-1}) is an important point to consider for the treatment of high-As AMD.

Despite the slight differences observed in the microbiology of the two bioreactors, the general performances (in terms of As and Fe oxidation and removal) were similar. The global stability of the system performances, (including both the temporal stability and the capacity to recover the performances after disturbances) may rely on functional redundancy of the bacterial communities. Indeed, different taxonomic groups sharing similar functions allowed the performance of a system to be maintained even when the community structure changes (Allison and Martiny, 2008). Thus, the robustness of the treatment system may rely both on the resilience capacity and the functional redundancy of the bacterial communities. This is in

line with the uncoupling between the resilience in function and the resilience in bacterial diversity described by Mills *et al.,* (2003).

Conclusion

Inside the bioreactors, FeOB were controlled by pH, dissolved Fe and As concentrations and temperature. The over-representation of *Ferrovum* in the active community, together with the positive correlation between its abundance and the highest treatment performances, confirmed its central role in the treatment efficiency. Furthermore, based on the positive correlation between its relative abundance and dissolved arsenic concentration, *Ferrovum* appeared particularly well adapted for the treatment of As rich effluents. *Leptospirillum* was another permanent member of the active community, which suggests its contribution to the stable performances. The bioreactor filled with wood and pozzolana (WP) showed a faster recovery of its performances after interruptions that may be attributed to a higher bacterial alpha diversity.

Our work provided the first evidence of the expression of the arsenite oxidase gene (*aioA*) in treatment bioreactors under field-conditions. This is an important function since As oxidation contributes to a more efficient removal of As, mainly under its more stable form (As(V)), which is a clear advantage for future application in bioremediation. More effort is required to optimize the quantification of *aioA* gene expression to better identify the factors regulating the expression of this key function.

The resilience of bacterial communities to operational disruptions and variability of the chemistry of the AMD of on-site treatment is another essential point in the perspective of a large-scale AMD treatment.

The validation of our process in real field conditions provided achievement of Technology Readiness Level 5. This technology, which did not use chemical reagent, could be competitive with lime treatment, provided that additional treatment step such as sulfate-reducing bioreactor is used to meet discharge standards.

Acknowledgments

The authors thank the ADEME for financial support [APR-GESIPOL-2017-COMPAs], the Occitanie region and the BRGM for co-funding of the PhD fellowship of Camila Diaz-Vanegas. We also acknowledge the OSU-OREME for co-funding the long-term monitoring of Carnoules AMD physico-chemistry. We thank Mickaël Charron (BRGM) for its technical assistance with the qPCR. We also thank Frédéric Mahé and Hervé Sanguin (MetaHealth metagenomic-based services (CIRAD, PHIM, Eco&Sols, Montpellier, France) for their expertise on metabarcoding and their helpful discussions.

References

Alam R, Mcphedran K (2019) Applications of biological sulfate reduction for remediation of arsenic – A review. Chemosphere 222:932–944. https://doi.org/10.1016/j.chemosphere.2019.01.194

Al-Amshawee S, Yunus MYBM, Lynam JG, Lee WH, Dai F, Dakhil IH (2021) Roughness and wettability of biofilm carriers: A systematic review. Environ Technol Innov 21:101233. https://doi.org/10.1016/j.eti.2020.101233

Allison S, Martiny J (2008) Resistance, resilience, and redundancy in microbial communities. PNAS 105: 11512-11519._https://doi.org/10.1073/pnas.080192510

Ahoranta SH, Kokko ME, Papirio S, Ozkaya B, Puhakka J (2016) Arsenic removal from acidic solutions with biogenic ferric precipitates. J Hazard Mater 306:124-132. https://doi.org/10.1016/j.jhazmat.2015.12.012

Afzal Ghauri M, Okibe N, Johnson BD (2007) Attachment of acidophilic bacteria to solid surfaces: The significance of species and strain variations. Hydrometallurgy 85:72–80. https://doi.org/10.1016/j.hydromet.2006.03.016

Asta MP, Ayora C, Román-Ross G, Cama J, Acero P, Gault AG, Charnock JM and Bardelli F (2010) Natural attenuation of arsenic in the Tinto Santa Rosa acid stream (Iberian Pyritic Belt, SW Spain): The role of iron precipitates. Chem Geol 271:1–12. https://doi.org/10.1016/j.chemgeo.2009.12.005

Bartsch S, Gensch A, Stephan S, Doetsch A, Gescher J (2017) Metallibacterium scheffleri: Genomic data reveal a versatile metabolism. FEMS Microbiol Ecol 93:1–10.

Bruneel O, Personné JC, Casiot C, Leblanc M, Elbaz-Poulichet F, Mahler BJ, Le Fléche A, Grimont PAD (2003) Mediation of arsenic oxidation by Thiomonas sp. in acid-mine drainage (Carnoulès, France). J Appl Microbiol 95:492–499. https://doi.org/10.1046/j.1365-2672.2003.02004.x

Campos-Quevedo N, Moreno-Perlin T, Razo-Flores E, Stams A, Celis L, Sanchez-Andrea I (2021) Acetotrophic sulfate-reducing consortia develop active biofilms on zeolite and glass beads in batch cultures at initial pH 3. Appl Microbiol Biotechnol 105:5213–5227. https://doi.org/10.1007/s00253-021-11365-0

Casiot C, Morin G, Juillot F, Bruneel O, Personné J-C, Leblanc M, Duquesne K, Bonnefoy V, Elbaz-Poulichet F (2003) Bacterial immobilization and oxidation of arsenic in acid mine drainage (Carnoulès creek, France). Water Research 37: 2929–2936. doi:10.1016/S0043-1354(03)00080-0

Chen LX, Li JT, Chen YT, Huang L, Hua Z, Hu M, Shu W (2013) Shifts in microbial community composition and function in the acidification of a lead/zinc mine tailings. Environ Microbiol 15:2431–2444. https://doi.org/10.1111/1462-2920.12114

Dave SR, Gupta KH, Tipre DR (2008) Characterization of arsenic resistant and arsenopyrite oxidizing *Acidithiobacillus ferrooxidan*s from Hutti gold leachate and effluents. Bioresour Technol 99:7514–7520. https://doi.org/10.1016/j.biortech.2008.02.019

De Caceres M, and Legendre P. (2009). Associations between species and groups of sites: indices and statistical inference. Ecology 90: 3566–3574. doi: 10.1890/ 08-1823.1

Diaz-Vanegas C, Casiot C, Lin C, De Windt L, Héry M, Desoeuvre A, Bruneel O, Battaglia-Brunet F, Jacob J (2022) Performance of semi‐passive systems for the biological treatment of high‐As acid mine drainage: Results from a year of monitoring at the Carnoulès mine (Southern France). Mine Water Environ 41: 679–694. https://doi.org/10.1007/ s10230-022-00885-4

Ebrahimi S, Fernández Morales FJ, Kleerebezem R, Heijnen J, van Loosdrecht M (2005) High-rate acidophilic ferrous iron oxidation in a biofilm airlift reactor and the role of the carrier material. Biotechnol Bioeng 90:462–472. https://doi.org/10.1002/bit.20448

Edgar RC, Haas BJ, Clemente JC, Quince C, Knight R (2011) UCHIME improves sensitivity and speed of chimera detection. Bioinformatics 27:2194–2200. https://doi.org/10.1093/ bioinformatics/btr381

Egal M, Casiot C, Morin G, Elbaz-Poulichet F, Cordier MA, Bruneel O (2010) An updated insight into the natural attenuation of As concentrations in Reigous Creek (southern France). Appl Geochem 25:1949–1957. https://doi.org/10.1016/j.apgeochem. 2010.10.012

Emerson D, Field EK, Chertkov O, Davenport KW, Goodwin L, Munk C, Nolan, Woyke T (2013) Comparative genomics of freshwater Fe-oxidizing bacteria: Implications for physiology, ecology, and systematics. Front Microbiol 4:1–17. https://doi.org/10.3389/fmicb.2013.00254

Farasin J, Koechler S, Varet H, Deschamps J, Dillies MA, Proux C, Erhardt M, Huber A, Jagla B, Briandet R, Coppée JY, Arsène-Ploetze F (2017) Comparison of biofilm formation and motility processes in arsenic-resistant Thiomonas spp. strains revealed divergent response to arsenite. Microb Biotechnol 10:789–803. https://doi.org/10.1111/1751-7915.12556

Feng K, Zhang Z, Cai W, Liu W, Xu M, Yin H, Wang A, He Z, Deng Y (2017) Biodiversity and species competition regulate the resilience of microbial biofilm community. Mol

Ecol 26:6170–6182. https://doi.org/10.1111/mec.14356

Fernandez-Rojo L, Casiot C, Laroche E, Tardy V, Bruneel O, Delpoux S, Desoeuvre A, Grapin G, Savignac J, Boisson, J Morin, G, Battaglia-Brunet F, Joulian C, Héry M (2019) A field-pilot for passive bioremediation of As-rich acid mine drainage. J Environ Manage 232:910–918. https://doi.org/10.1016/j.jenvman.2018.11.116

Fernandez-Rojo L, Casiot C, Tardy V, Laroche E, Le Pape P, Morin G, Joulian C, Battaglia-Brunet F, Braungardt C, Desoeuvre A, Delpoux S, Boisson J, Héry M (2018) Hydraulic retention time affects bacterial community structure in an As-rich acid mine drainage (AMD) biotreatment process. Appl Microbiol Biotechnol 102:9803–9813. https://doi.org/10.1007/s00253-018-9290-0

Fernandez-Rojo L, Héry M, Le Pape P, Desoeuvre A, Torres E, Tardy V, Resongles E, Laroche E, Delpoux S, Joulian C, Battaglia-Brunet F, Boisson J, Grapin G, Morin G et Casiot C (2017) Biological attenuation of arsenic and iron in a continuous flow bioreactor treating acid mine drainage (AMD). Water Res 123:594–606. https://doi.org/10.1016/j.watres.2017.06.059

Fleming EJ, Cetinić I, Chan CS, King DW, Emerson D (2014) Ecological succession among iron-oxidizing bacteria. ISME J 8:804–815. https://doi.org/10.1038/ismej.2013.197

Florence K, Sapsford DJ, Johnson DB, Kay CM, Wolkersdorfer C (2016) Iron-mineral accretion from acid mine drainage and its application in passive treatment. Environ Technol (United Kingdom) 37:1428–1440. https://doi.org/10.1080/09593330.2015.1118558

Galili T, O'Callaghan A, Sidi J, Sievert C (2017) heatmaply: an R package for creating interactive cluster heatmaps for online publishing, Bioinformatics, 34:1600-1602 https://doi.org/10.1093/bioinformatics/btx657

Gavrilov SN, Korzhenkov AA, Kublanov IV, Bargiela R, Zamana LV, Popova AA, Toshchavoq SV, Golyshin PN, Golyshina O (2019) Microbial communities of polymetallic deposits' acidic ecosystems of continental climatic zone with high temperature contrasts. Front Microbiol 10:1573. https://doi.org/10.3389/fmicb.2019.01573

Grettenberger CL, Havig JR, Hamilton TL (2020) Metabolic diversity and co-occurrence of multiple *Ferrovum* species at an acid mine drainage site. BMC Microbiol 20:1–14. https://doi.org/10.1186/s12866-020-01768-w

Grossart HP (2010) Ecological consequences of bacterioplankton lifestyles: changes in concepts are needed. Environ Microbiol Rep. 2(6):706-14. doi: 10.1111/j.1758-

2229.2010.00179.x.

Hedrich S, Johnson DB (2012) A modular continuous flow reactor system for the selective bio-oxidation of iron and precipitation of schwertmannite from mine-impacted waters. Bioresour Technol 106:44–49. https://doi.org/10.1016/j.biortech.2011.11.130

Heinzel E, Janneck E, Glombitza F, Schlömann M, Seifert J (2009) Population dynamics of Iron-oxidizing communities in pilot plants for the treatment of acid mine waters. Environ Sci Technol 43: 6138–6144. doi: 10.1021/es900067d

Héry M, Casiot C, Resongles E, Gallice Z, Bruneel O, Desoeuvre A, Delpoux S (2014) Release of arsenite, arsenate and methyl-arsenic species from streambed sediment affected by acid mine drainage: A microcosm study. Environ Chem 11:514–524

Hovasse A, Bruneel O, Casiot C, Desoeuvre A, Farasin J, Héry M, Van Dorssealaer A, Carapito C, Arsene-Ploetze F (2016) Spatio-temporal detection of the Thiomonas population and the Thiomonas arsenite oxidase involved in natural arsenite attenuation processes in the Carnoulès acid mine drainage. Front Cell Dev Biol 4:3. https://doi.org/10.3389/fcell.2016.00003

Huq ME, Fahad S, Shao Z, Sarven MS, Khan IA, Alam M, Saeed M, Ullah H, Adnan M, Saud S, Cheng Q, Shaukait A, Wahid F, Zahim M, Raza MA, Saeed B, Riaz M, Khlan WU (2020) Arsenic in a groundwater environment in Bangladesh: Occurrence and mobilization. J Environ Manage 262:110318. https://doi.org/10.1016/j.jenvman.2020.110318

Jin D, Wang X, Liu L, Liang J, Zhou L (2020) A novel approach for treating acid mine drainage through forming schwertmannite driven by a mixed culture of Acidiphilium multivorum and Acidithiobacillus ferrooxidans prior to lime neutralization. J Hazard Mater 400:123108. https://doi.org/10.1016/j.jhazmat.2020.123108

Johnson DB, Hallberg KB, Hedrich S (2014) Uncovering a microbial enigma: isolation and characterization of the streamer-generating, iron-oxidizing, acidophilic bacterium "*Ferrovum myxofaciens*." Appl Environ Microbiol 80:672–680. https://doi.org/10.1128/AEM.03230-13

Jones DS, Kohl C, Grettenberger C, Larson L, Burgos W, Macalady J (2015) Geochemical niches of iron-oxidizing acidophiles in acidic coal mine drainage. Appl Environ Microbiol 81:1242–1250. https://doi.org/10.1128/AEM.02919-14

Kay CM, Rowe OF, Rocchetti L, Coupland K, Hallberg K, Johnson B (2013) Evolution of microbial "Streamer" growths in an acidic, metal-contaminated stream draining an

abandoned underground copper mine. Life 3:189–210. https://doi.org/10.3390/life3010189

Kinnunen PHM, Puhakka JA (2004) High-rate ferric sulfate generation by a L*eptospirillium ferriphilum* dominated biofilm and the role of jarosite in biomass retainment in a fluidized-bed reactor. Biotechnol Bioeng 85:697–705. https://doi.org/10.1002/bit.20005

Kwon S, Kim TS, Yu GH, Jung JH, Park HD (2010) Bacterial community composition and diversity of a full-scale integrated fixed-film activated sludge system as investigated by pyrosequencing. J Microbiol Biotechnol 20(12):1717-23.

Lane DJ (1991) 16S/23S rRNA Sequencing. In: Stackebrandt, E. and Goodfellow, M., Eds., Nucleic Acid Techniques in Bacterial Systematic, John Wiley and Sons, New York, 115-175.

Laroche E, Casiot C, Fernandez-Rojo L, Desoeuvre A, Tardy V, Bruneel O, Battaglia-Brunet F, Joulian C, Héry M (2018) Dynamics of bacterial communities mediating the treatment of an As-rich acid mine drainage in a field pilot. Front Microbiol 9:1–13. https://doi.org/10.3389/fmicb.2018.03169

Leblanc M, Achard B, Ben Othman D, Luck JM (1996) Accumulation of arsenic from acidic mine waters by ferruginus bacterial accretions (stromatolites). Appl Geochemistry 11:541–554

Li L, Liu Z, Zhang M, Meng D, Liu X, Wang P, Li X, Jiang Z, Zhong S, Jiang C, Yin H (2020) Insights into the metabolism and evolution of the genus Acidiphilium, a typical acidophile in Acid Mine Drainage. mSystems. 17;5(6):e00867-20. doi: 10.1128/mSystems.00867-20.

Li Y, Chen W, Zheng X, Liu Q, Xiang W, Qu J, Yang C (2021) Microbial community structure analysis in a hybrid membrane bioreactor via high-throughput sequencing. Chemospher 282:130989. doi: 10.1016/j.chemosphere.2021.130989Lopez-Ponnada EV, Lynn TJ, Peterson M, Ergas SJ, Mihelcic JR (2017) Application of denitrifying wood chip bioreactors for management of residential non-point sources of nitrogen. J Biol Eng 11:1–14. https://doi.org/10.1186/s13036-017-0057-4

Macías F, Caraballo MA, Nieto JM, Rotting T, Ayora C (2012) Natural pretreatment and passive remediation of highly polluted acid mine drainage. J Environ Manage 104:93–100. https://doi.org/10.1016/j.jenvman.2012.03.027

Mahé F, Czech L, Stamatakis A, Quince C, de Vargas C, Dunthorn M, Rognes T (2021) Swarm v3: towards tera-scale amplicon clustering. Bioinformatics 38:267–269.

https://doi.org/10.1093/bioinformatics/btab493

Maillot F, Morin G, Juillot F, Bruneel O, Casiot C, Ona-Nguema G, Wang Y, Lebrun S, Qubry E, Vlaic G, Brozn GE (2013) Structure and reactivity of As(III)- and As(V)-rich schwertmannites and amorphous ferric arsenate sulfate from the Carnoulès acid mine drainage, France: Comparison with biotic and abiotic model compounds and implications for As remediation. Geochim Cosmochim Acta 104:310–329. https://doi.org/10.1016/j.gca.2012.11.016

Martin M (2013) Cutadapt removes adapter sequences from high-throughput sequencing reads. EMBnet.journal 7:2803–2809

McMurdie PJ, Holmes S (2013) phyloseq: an R package for reproducible interactive analysis and graphics of microbiome census data. PloS One 8, e61217.

Méndez-García C, Mesa V, Sprenger RR, Richter M, Suaréz M, Solano J, Bargiela R, Golyshina O V, Manteca A, Ramos JL, Gallego JR, Llorente I, Martins dos Santos V AP, Jensen ON, Pelaez AI, Sanchez J, Ferrer M (2014) Microbial stratification in low pH oxic and suboxic macroscopic growths along an acid mine drainage. ISME J 8:1259–1274. https://doi.org/10.1038/ismej.2013.242

Méndez-García C, Peláez AI, Mesa V, Sánchez J, Golyshina OV, Ferrer M (2015) Microbial diversity and metabolic networks in acid mine drainage habitats. Front Microbiol 6:1–17. https://doi.org/10.3389/ fmicb.2015.00475

Michel C, Jean M, Coulon S, Dictor M.-C Delorme F, Morin D, Garrido F (2007) Biofilms of As(III)-oxidising bacteria: Formation and activity studies for bioremediation process development. Appl Microbiol Biotechnol 77:457–467. https://doi.org/10.1007/s00253-007-1169-4

Mills A, Herman J, Hornberger G, Ford R (2003) Functional redundancy promotes functional stability in diverse microbial bioreactor communities. SAE Technical Paper 2003-01-2509

Morin G, Juillot F, Casiot C, Bruneel O, Personné JC, Elbaz-Poulichet F, Leblanc M, Ildefonse P, Calas G (2003) Bacterial Formation of Tooeleite and Mixed Arsenic(III) or Arsenic(V)−Iron(III) Gels in the Carnoulès Acid Mine Drainage, France. A XANES, XRD, and SEM Study. Environ Sci Technol 37: 1705–1712. doi:10.1021/es025688p

Oksanen J, Blanchet FG, Friendly M, Kindt R, Legendre P, McGlinn D, Minchin PR, O'Hara RB, Simpson GL, Solymos P, Henry M, Stevens H, Szoecs E, Wagner H (2018) vegan: community ecology package, R pack- age version 2.5-3.

Paikaray S (2015) Arsenic geochemistry of acid mine drainage. Mine Water Environ 34:181–

196. https://doi.org/10.1007/s10230-014-0286-4

Pereira MA, Alves MM, Azeredo J, Mota M, Oliveira R (2000) Influence of physico-chemical properties of porous microcarriers on the adhesion of an anaerobic consortium. J Ind Microbiol Biotechnol 24:181–186. https://doi.org/10.1038/sj.jim.2900799

Plewniak F, Koechler S, Le Paslier D, Héry M, Bruneel O, Bertin P (2020) In situ metabolic activities of uncultivated Ferrovum sp. CARN8 evidenced by metatranscriptomic analysis. Res Microbiol 171:37–43. https://doi.org/10.1016/j.resmic.2019.09.008

Quast C, Pruesse E, Yilmaz P, Gerken J, Schweer T, Yarza P, Peplies J, Glockner F (2013) The SILVA ribosomal RNA gene database project: Improved data processing and web-based tools. Nucleic Acids Res 41:590–596. https://doi.org/10.1093/nar/gks121

Quéméneur M, Cébron A, Billard P, Battaglia-Brunet F, Garrido F, Leyval C, Joulian C (2010) Population structure and abundance of arsenite-oxidizing bacteria along an arsenic pollution gradient in waters of the upper isle river basin, France. Appl Environ Microbiol 76:4566–4570. https://doi.org/ 10.1128/AEM.03104-09

Quéméneur M (2008) Les processus biogéochimiques impliqués dans la mobilité de l'arsenic: recherche de bioindicateurs. PhD thesis, Nancy University, 21st November 2008.

Quéméneur M, Heinrich-Salmeron A, Muller D, Lièvremont D, Jauzein M, Bertin P, Garrido F, Joulian C (2008) Diversity surveys and evolutionary relationships of aoxB genes in aerobic arsenite-oxidizing bacteria. Appl Environ Microbiol 74:4567–4573. https://doi.org/10.1128/AEM.02851-07

R Core Team (2018) R: A Language and Environment for Statistical Computing. R Foundation for Statistical Computing, Vienna. https://www.R-project.org

Resongles E, Casiot C, Freydier R, Dezileau L, Viers J, Elbaz-Poulichet (2014) Persisting impact ofhistorical mining activity to metal (Pb, Zn, Cd, Tl, Hg) and metalloid (As, Sb) enrichment in sediments of the Gardon River, Southern France. Sci Total Environ 481:509–521. https://doi.org/10.1016/j.scitotenv.2014.02.078

Resongles E, Casiot C, Freydier R, Le Gall M, Elbaz-Poulichet F (2015) Variation ofdissolved and particulate metal(loid) (As, Cd, Pb, Sb, Tl, Zn) concentrations under varying discharge during a Mediterranean flood in a former mining watershed, the Gardon River (France). J Geochemical Exploration 158: 132-142. https://doi.org/10.1016/j.gexplo.2015.07.010

Rezaie B, Anderson A (2020) Sustainable resolutions for environmental threat of the acid mine drainage. Sci Total Environ 717:137211.

https://doi.org/10.1016/j.scitotenv.2020.137211

Rognes T, Flouri T, Nichols B, Quince C, Mahé F (2016) VSEARCH: a versatile open source tool for metagenomics. PeerJ 18;4:e2584. doi: 10.7717/peerj.2584.

Sheng Y, Bibby K, Grettenberger C, Kaley B, Macalady J, Wang G, Burgos W (2016) Geochemical and temporal influences on the enrichment of acidophilic iron-oxidizing bacterial communities. Appl Environ Microbiol 82:3611–3621. https://doi.org/10.1128/AEM.00917-16

Sheng Y, Kaley B, Bibby K, Grettenberger C, Macalady J, Wang G, Burgos W (2017) Bioreactors for low-pH iron(II) oxidation remove considerable amounts of total iron. RSC Adv 7:35962–35972. https://doi.org/10.1039/c7ra03717a

Sonthiphand P, Rattanaroongrot P, Mek-Yong K, Kusonmano K, Rangsiwutisak C, Uthaipaisanwong P, Chotpantarat S, Termsaithong T (2021) Microbial community structure in aquifers associated with arsenic: analysis of 16S rRNA and arsenite oxidase genes. PeerJ 9:1–29. https://doi.org/10.7717/peerj.10653

Tang X, Chao J, Gong Y, Wang Y, Wilhelm SW, Gao G (2017) Spatiotemporal dynamics of bacterial community composition in large shallow eutrophic Lake Taihu: High overlap between free-living and particle-attached assemblages. Limnology and Oceanography, 62(4), 1366-1382.Tardy V, Casiot C, Fernandez-Rojo L, Resongles E, Desoeuvre A, Joulian C, Battaglia-Brunet, Héry M (2018) Temperature and nutrients as drivers of microbially mediated arsenic oxidation and removal from acid mine drainage. Appl Microbiol Biotechnol 102:2413–2424. https://doi.org/10.1007/s00253-017-8716-4

Tufano KJ, Fendorf S (2008) Confounding impacts of iron reduction on arsenic retention. Environ Sci Technol 42:4777–4783. https://doi.org/10.1021/es702625e

Tyagi M, da Fonseca MMR, de Carvalho CCCR (2011) Bioaugmentation and biostimulation strategies to improve the effectiveness of bioremediation processes. Biodegradation 22:231–241. https://doi.org/10.1007/s10532-010-9394-4

Volant A, Bruneel O, Desoeuvre A, Héry M, Casiot C, Bru N, Delpoux S, Fahy A, Javerliat F, Bouchez O, Bertin P, Elbaz-Poulichet F, Lauga B (2014) Diversity and spatiotemporal dynamics of bacterial communities: Physicochemical FEMS Microbiol Ecol 90:247–263. https://doi.org/10.1111/1574-6941.12394

Wang S, Wang X, Zhang C, Zhang C, Li F, Guo G (2016) Bioremediation of oil sludge contaminated soil by landfarming with added cotton stalks. Int Biodeterior Biodegrad 106:150–156. https://doi.org/10.1016/j.ibiod.2015.10.014

Wang M, Zhou L (2012) Simultaneous oxidation and precipitation of iron using jarosite

immobilized Acidithiobacillus ferrooxidans and its relevance to acid mine drainage. Hydrometallurgy 125–126:152–156. https://doi.org/10.1016/j.hydromet.2012.06.003

Weisburg WG, Barns SM, Pelletier DA, Lane DJ (1991) 16S ribosomal DNA amplification for phylogenetic study. J Bacteriol. 173(2):697-703. doi: 10.1128/jb.173.2.697-703.1991.

Wickham H (2017). tidyverse: Easily Install and Load the 'Tidyverse'. R package version 1.2.1. https://CRAN.R-project.org/package=tidyverse

Wickham H, François R, Henry L, Müller K (2022) dplyr: A Grammar of Data Manipulation, R package version 1,0,9, https://CRAN,R-project,org/package=dplyr

Zhao Y, Liu D, Huang W, Yang Y, Ji M, Duc Nghiem L, Thang QT, Tran NH (2019) Insights into biofilm carriers for biological wastewater treatment processes: Current state-of-the-art, challenges, and opportunities. Bioresour Technol 288:121619. https://doi.org/10.1016/j.biortech.2019.121619

Zhu L, Yuan H, Shi Z, Deng L, Yu Z, Li Y, He Q (2022) Metagenomic insights into the effects of various biocarriers on moving bed biofilm reactors for municipal wastewater treatment. Science of The Total Environment 813: 151904

Ziegler S, Dolch K, Geiger K, Krause S, Asskamp M, Eusterhues K, Kriews M, Wilhems-Dick, Goettlicher J, Mazlan J, Gescher J (2013) Oxygen-dependent niche formation of a pyrite-dependent acidophilic consortium built by archaea and bacteria. ISME J 7:1725–1737. https://doi.org/10.1038/ismej.2013.64

Figure 1. Evolution of the bioreactor performances (represented by KOFe and As precipitation rate). Solid lines represent the evolution of the kinetic constant value (KOFe) for the WP and PS bioreactors. Dashed lines represent the evolution of the arsenic precipitation rates (mol L^{-1} s^{-1}) calculated for each pilot. The triangles and the squares represent the data from the PS and WP bioreactor respectively (Diaz-Vanegas et al., 2022). The stars represent the periods with the clogging of the air diffusers. The values used for this graph correspond to the average of the data obtained for each period.

Figure 2. Diversity indices for the total bacterial communities developed in PS and WP bioreactors; alpha diversity: Chao1 and Shannon (a), beta diversity (Bray-Curtis) (b). ("****" =p-value < 0.0001, "***" p-value <0.001). These analyses include total and active communities.

Figure 3. NMDS with the main taxa (genus level) explaining the communities' differences (p-value < 0.05). When genus identification was not possible, classification was made at the family or at the order level. The symbols represent the structure of the bacterial communities of each sample. The shape of the symbol represents the lifestyle (suspended or attached) and the status of the community (total community based on DNA analysis or active community based on RNA analysis). The colors represent the periods of monitoring (B, C, D, E, F and G). The two ellipses differentiate the samples from each bioreactor (dashed line for the WP samples and solid line for the PS samples). Stress value= 0.2088535.

Figure 4. Evolution of the relative abundances of the main bacterial at genus level (relative abundance > 0.05 % of total number of sequences) over the monitoring periods. The results are presented for the PS (plastic biomass carrier) and WP (wood and pozzolana as biomass carrier) bioreactors according to the different lifestyle (attached versus suspended) and to the status of the communities (total or active). When genus identification was not possible, classification was made at the family level (∗) or at the order level (∗∗).

Figure 5. Abundance of genes and transcripts in the biogenic precipitates and in the water collected at the inlet and at the outel of the two bioreactors (average of all the periods). 16S rRNA genes and transcripts in the attached community (a), and in the suspended community (b), *aioA* genes and transcripts in the attached community (c) and in the suspended community (d). Analyses were performed on DNA (presence of the genetic potential) and cDNA (gene expression). Values annotated with the same letter are not significantly different (Tukey's multiple range test with p = 0.05). The quantification of the *aioA* transcripts from cDNA in the WP biogenic precipitates was below the detection limit.

Figure 6. *aioA* / 16S rRNA genes ratio in the suspended (outlet water) and attached communities (biogenic precipitates) in the two bioreactors (based on DNA analyses only). Data are mean values (n= 3). *** the three asterisks correspond to period F (bioreactor PS and WP) and period G (only bioreactor PS), for which data are missing due to technical limitations.

Figure 7. Heat map of the Spearman correlation coefficients between relative abundance of the most dominant taxa (vertical axis) and physicochemical parameters of the inlet water, operational parameters or performances indicators (represented in the horizontal axis). All the parameters used are presented in **Error! Reference source not found.**, supplementary Table S1 and S2; for the performance indicators only the periods with optimal performances B- E were considered. Correlation analyses were performed with the sum of the sequences data from the total and active communities (based on DNA and RNA analyses). The last group corresponds to the relative abundance of the As(III)-oxidizing bacteria (correlation performed only with the abundance of the total communities (based on DNA analyses). When genus identification was not possible, classification was made at the family level (∗) or at the order level (∗∗).

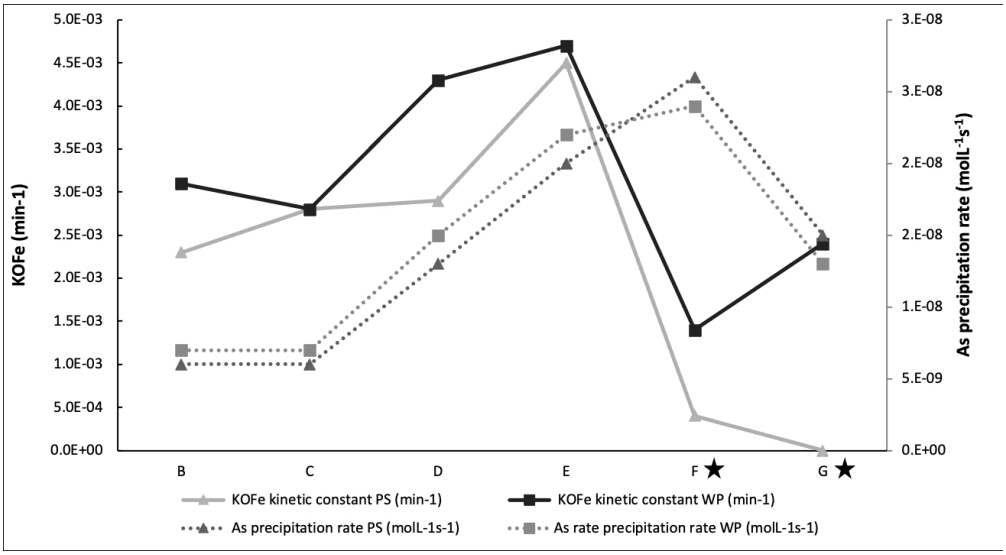

Figure 1. Evolution of the bioreactor performances (represented by KOFe and As precipitation rate). Solid lines represent the evolution of the kinetic constant value (KOFe) for the WP and PS bioreactors. Dashed lines represent the evolution of the arsenic precipitation rates (mol L-1 s-1) calculated for each pilot. The triangles and the squares represent the data from the PS and WP bioreactor respectively (Diaz-Vanegas et al., 2022). The stars represent the periods with the clogging of the air diffusers. The values used for this graph correspond to the average of the data obtained for each period

221x121mm (150 x 150 DPI)

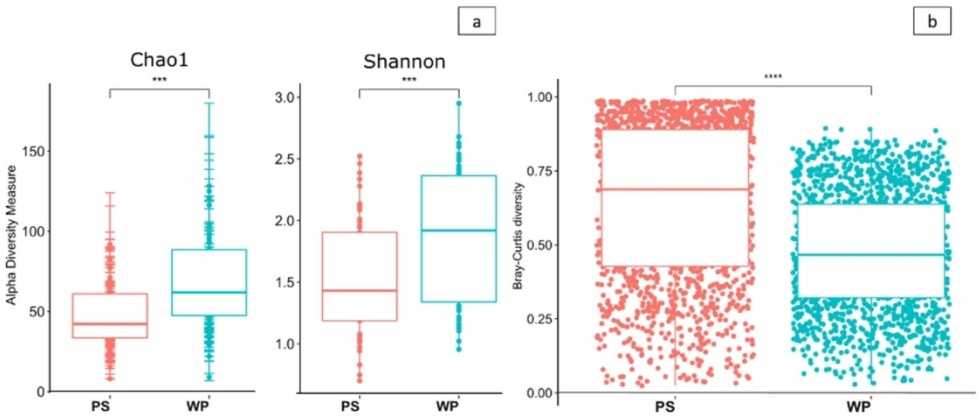

Figure 2. Diversity indices for the total bacterial communities developed in PS and WP bioreactors; alpha diversity: Chao1 and Shannon (a), beta diversity (Bray-Curtis) (b). ("****" =p-value < 0.0001, "***" p-value <0.001). These analyses include total and active communities.

260x107mm (150 x 150 DPI)

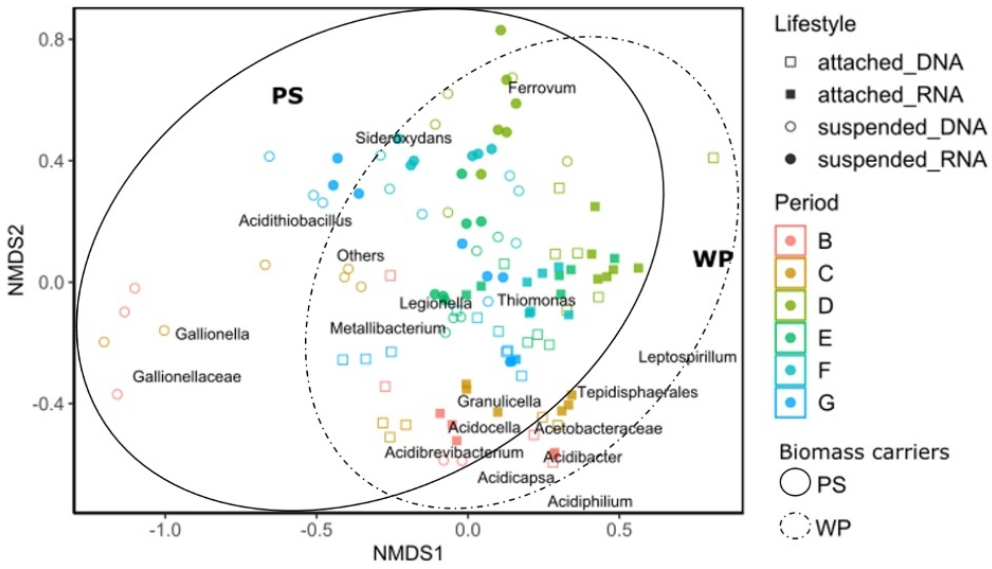

Figure 3. NMDS with the main taxa (genus level) explaining the communities' differences (p-value < 0.05). When genus identification was not possible, classification was made at the family or at the order level. The symbols represent the structure of the bacterial communities of each sample. The shape of the symbol represents the lifestyle (suspended or attached) and the status of the community (total community based on DNA analysis or active community based on RNA analysis). The colors represent the periods of monitoring (B, C, D, E, F and G). The two ellipses differentiate the samples from each bioreactor (dashed line for the WP samples and solid line for the PS samples). Stress value= 0.2088535.

160x90mm (150 x 150 DPI)

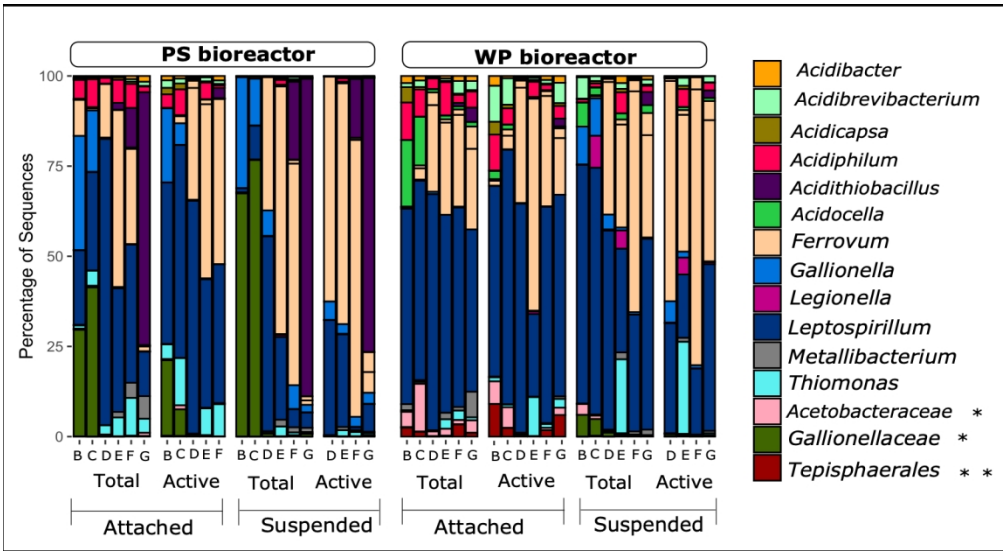

Figure 4. Evolution of the relative abundances of the main bacterial at genus level (relative abundance > 0.05 % of total number of sequences) over the monitoring periods. The results are presented for the PS (plastic biomass carrier) and WP (wood and pozzolana as biomass carrier) bioreactors according to the different lifestyle (attached versus suspended) and to the status of the communities (total or active). When genus identification was not possible, classification was made at the family level (*) or at the order level (**).

278x152mm (150 x 150 DPI)

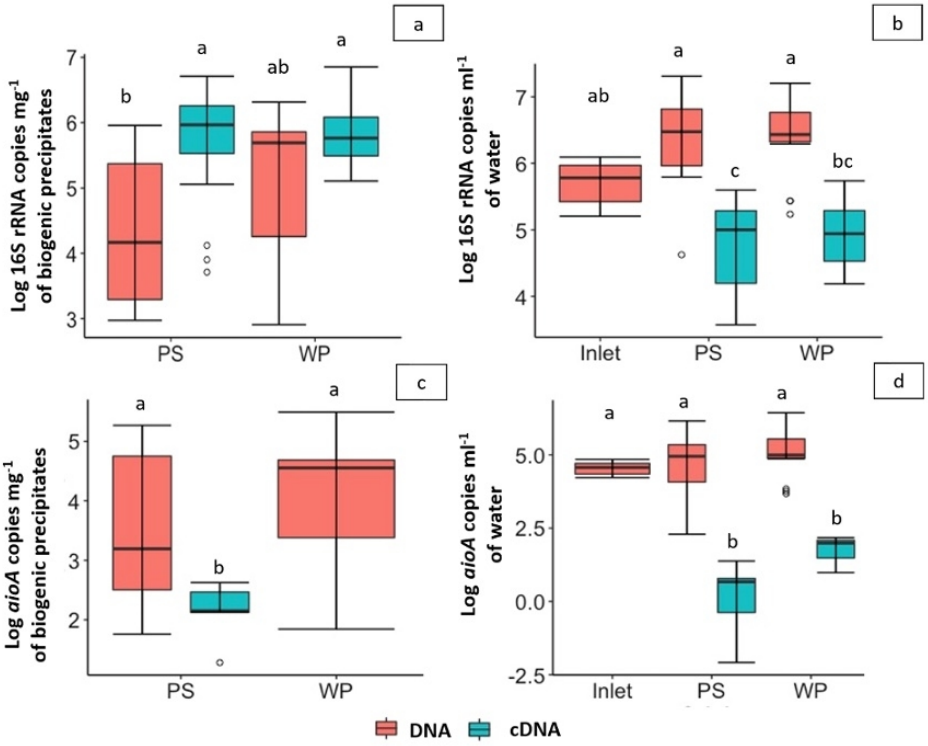

Figure 5. Abundance of genes and transcripts in the biogenic precipitates and in the water collected at the inlet and at the outel of the two bioreactors (average of all the periods). 16S rRNA genes and transcripts in the attached community (a), and in the suspended community (b), aioA genes and transcripts in the attached community (c) and in the suspended community (d). Analyses were performed on DNA (presence of the genetic potential) and cDNA (gene expression). Values annotated with the same letter are not significantly different (Tukey's multiple range test with p = 0.05). The quantification of the aioA transcripts from cDNA in the WP biogenic precipitates was below the detection limit.

154x121mm (150 x 150 DPI)

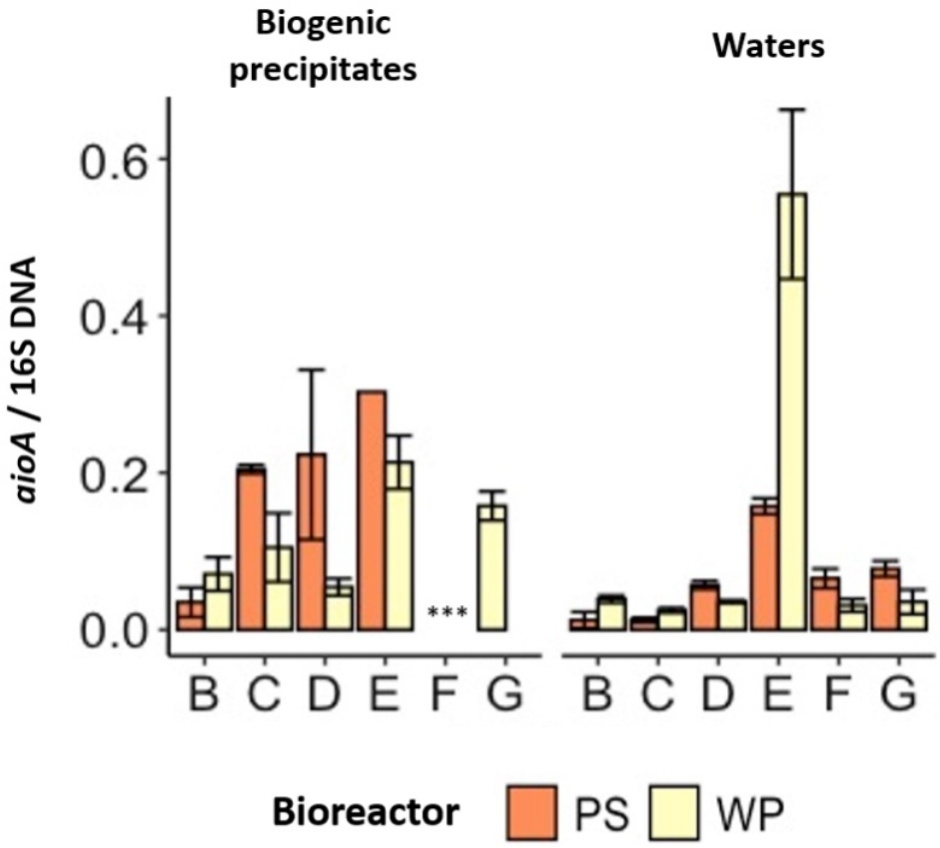

Figure 6. aioA / 16S rRNA genes ratio in the suspended (outlet water) and attached communities (biogenic precipitates) in the two bioreactors (based on DNA analyses only). Data are mean values (n= 3). *** the three asterisks correspond to period F (bioreactor PS and WP) and period G (only bioreactor PS), for which data are missing due to technical limitations.

140x126mm (150 x 150 DPI)

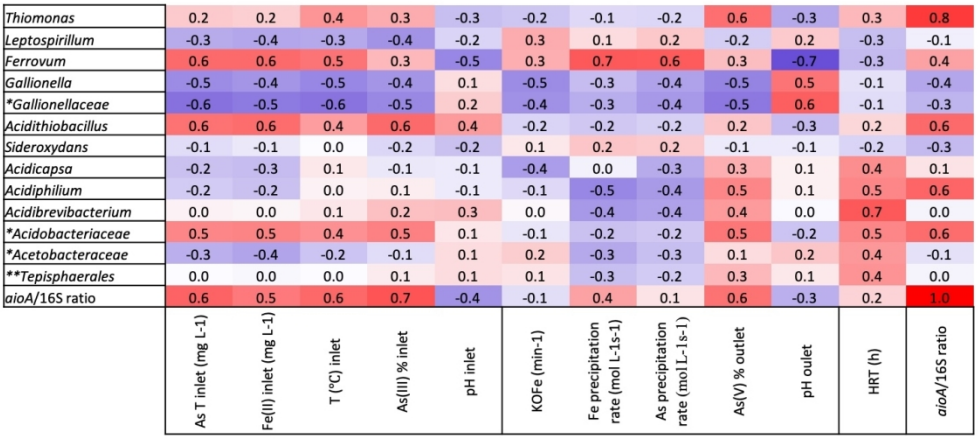

Figure 7. Heat map of the Spearman correlation coefficients between relative abundance of the most dominant taxa (vertical axis) and physicochemical parameters of the inlet water, operational parameters or performances indicators (represented in the horizontal axis). All the parameters used are presented in Table 1, supplementary Table S1 and S2; for the performance indicators only the periods with optimal performances B- E were considered. Correlation analyses were performed with the sum of the sequences data from the total and active communities (based on DNA and RNA analyses). The last group corresponds to the relative abundance of the As(III)-oxidizing bacteria (correlation performed only with the abundance of the total communities (based on DNA analyses). When genus identification was not possible, classification was made at the family level (∗) or at the order level (∗∗).

250x117mm (150 x 150 DPI)

Table 1 Inlet and outlet water main characteristics (DO was measured inside the bioreactor)

Date (d.m.y)	Period	T (°C)	pH inlet	As T* inlet (mg L^{-1})	Fe (II) inlet (mg L^{-1})	HRT (h)		TOC (mg L^{-1})		DO (mg L^{-1})**	
						PS	WP	PS	WP	PS	WP
19.12.19	B	13.9	4.82	53.64	501	18	19	2.3	5.4	NA	NA
06.02.20	C	8.3	4.11	49.5	448.9	18	19	3.0	3.5	10.7	NA
12.03.20	D	14.1	3.87	70.7	665.2	9	10	2.9	3.0	9.1	10.0
18.06.20	E	22.3	3.79	88.1	732.3	18	19	NA	NA	6.1	5.0
27.07.20	F	20.2	4.12	93.1	820.7	9	10	4.0	4.6	0.2	3.1
15.09.20	G	20.5	4.44	91.0	768.6	18	19	4.6	4.1	NA	NA

*Total As; **Dissolved Oxygen measured inside the bioreactors

Supplementary Information

Table SI 1. Chemical characterization of inlet and outlet waters for the sampling dates where microbioligical analyses were performed

Date (dd.mm.yy)	Period	Flow rate ($L \cdot h^{-1}$)	HRT (h)		pH inlet	Temp. (°C)	As T inlet* $mg \cdot L^{-1}$	Fe (II) inlet $mg \cdot L^{-1}$	As(III) inlet %	KOFe (min^{-1})		Fe rate prec. ($mol \cdot L^{-1} s^{-1}$)		As removal ratio ($mol \cdot L^{-1} s^{-1}$)		As(V) outlet %		TOC** outlet ($mg \cdot L^{-1}$)	
			PS	WP						PS	WP	PS	WP	PS	WP	PS	WP	PS	WP
19.12.19	B	15	17.5	19.3	4.82	13.9	53.64	501	73	2.50 E-03	3.30 E-03	6.20 E-08	5.80 E-08	3.60 E-04	2.10 E-04	9.7	34.5	2.32	5.44
06.02.20	C	15	17.5	19.3	4.11	8.3	49.5	448.9	71	2.20 E-03	2.90 E-03	4.90 E-08	5.40 E-08	3.80 E-04	2.26 E-04	38.4	40.3	3.03	3.54
12.03.20	D	30	8.8	9.7	3.87	14.1	70.7	665.2	71	2.90 E-03	4.60 E-03	1.30 E-07	1.30 E-07	9.80 E-04	6.70 E-04	20.2	13.9	2.89	3.01
18.06.20	E	15	17.5	19.3	3.79	22.3	88.1	732.3	80	2.75 E-03	3.00 E-03	1.20 E-07	1.25 E-07	3.30 E-04	2.10 E-04	61.2	96.5	NA	NA
27.07.20	F	30	8.8	9.7	4.12	20.2	93.1	820.7	78	3.54 E-04	1.50 E-03	3.20 E-09	1.04 E-07	8.60 E-04	6.90 E-04	27.9	19.5	4.02	4.61
15.09.20	G	15	17.5	19.3	4.44	20.5	91.0	768.6	82	1.20 E-03	2.30 E-03	5.80 E-08	7.10 E-08	3.90 E-04	3.30 E-04	78.9	87.5	4.56	4.13

*Total As ; **Total Organic Carbon

Table SI 2. Performance indicators for the sampling dates where microbiological analyses were performed

Date (d.m.y)	Period	Total As (wt%)		Total Fe (wt%)		As/Fe (mol mol-1)*		%As V (wt%)	
		PS	WP	PS	WP	PS	WP	PS	WP
19.12.19	B	10.7	4.9	37	22	0.39	0.30	81	88
06.02.20	C	NA	NA	NA	NA	NA	NA	NA	NA
12.03.20	D	9.1	5.7	36	28	0.34	0.27	69	53
18.06.20	E	8.6	8.3	36	32	0.32	0.35	77	78
27.07.20	F	8.3	5.0	31	25	0.36	0.26	83	83
15.09.20	G	12.2	8.4	33	25	0.49	0.45	92	94

*Molar ratio

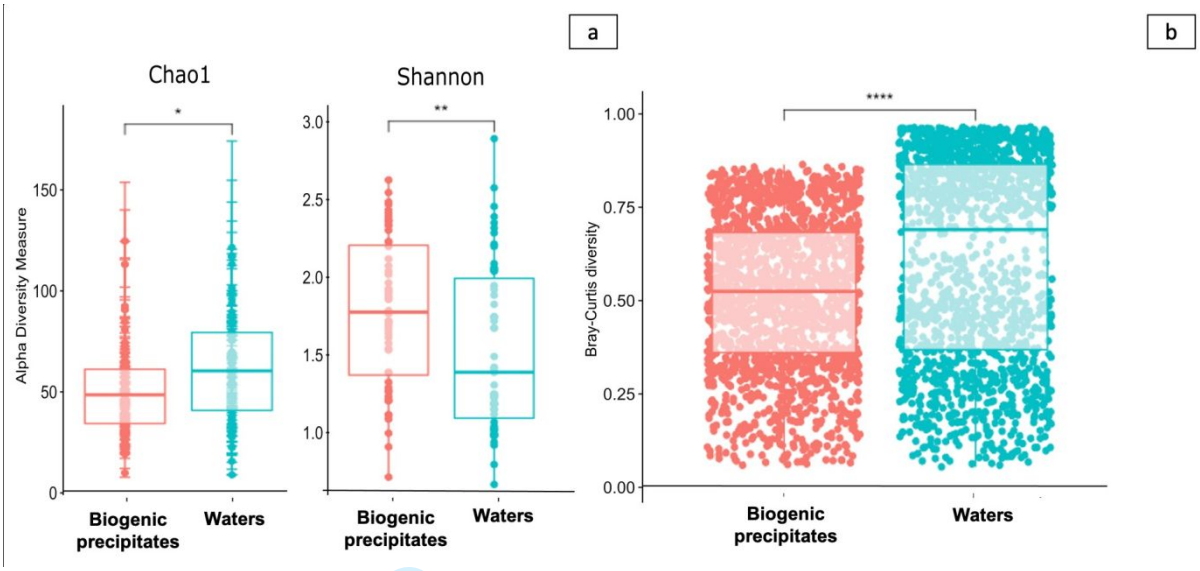

Figure SI 1. Indices of alpha (a) and beta (b) diversity obtained from the different types of samples (biogenic precipitates and water). ("****" =p-value < 0.0001, "***" p-value < 0.001, "**"= p-value < 0.01, "*"= p-value < 0.05). These analyses include total and active.

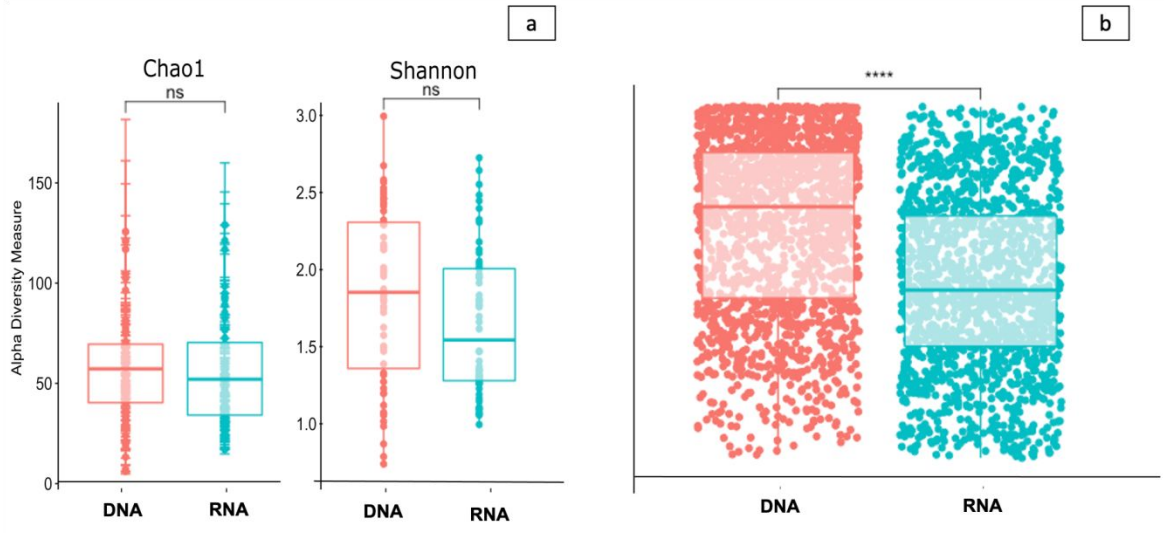

Figure SI 2. Indices of alpha (a) and beta (b) diversity obtained from the DNA and RNA extracts. ("****" =p-value < 0.0001, "ns" = p-value > 0.05).

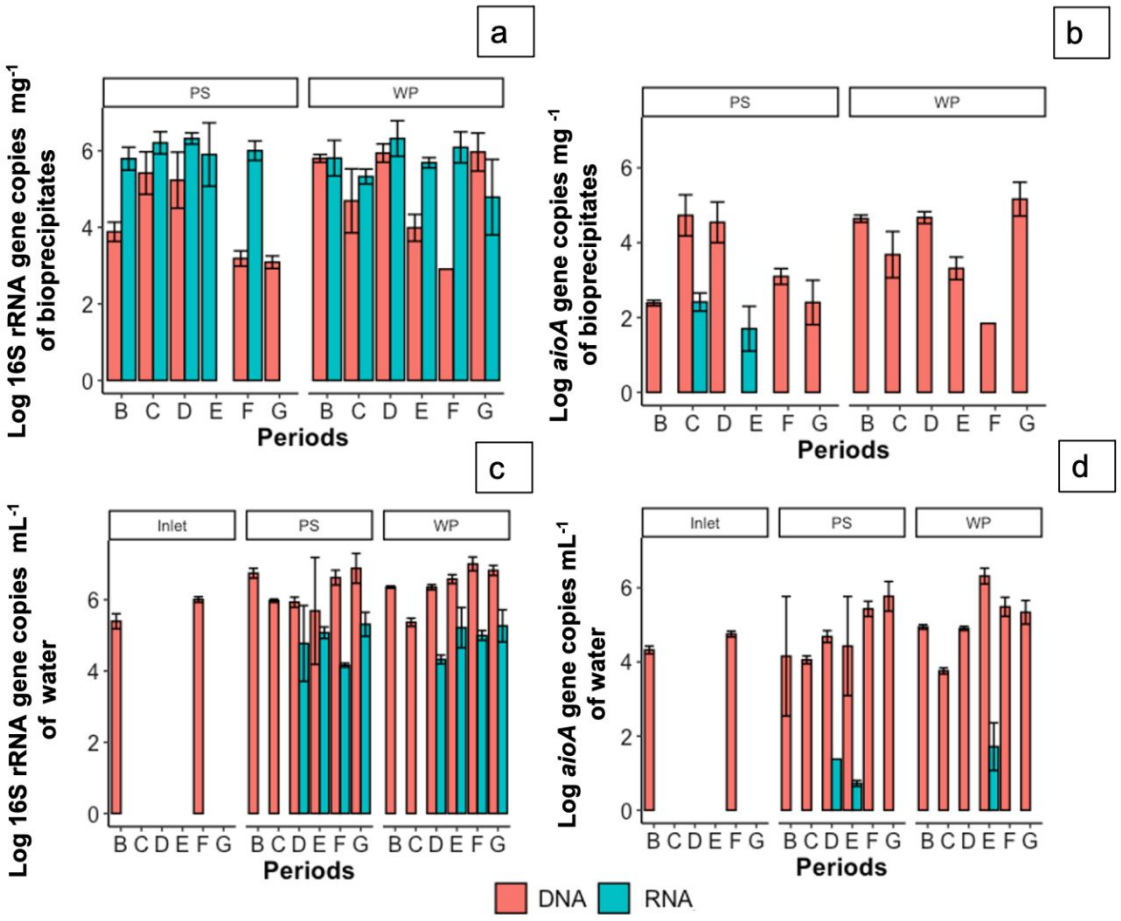

Figure SI 3. Number of copies of 16S rRNA gene (a) and *aioA* gene (b) in biogenic precipitates. Number of copies of 16S rRNA gene (c) and *aioA* gene (d) in water.